A THESIS SUBMITTED TO
THE GRADUATE SCHOOL OF NATURAL AND APPLIED SCIENCES
OF ÇANKIRI KARATEKİN UNIVERSITY

DESIGN OF POWER GENERATION SYSTEM USING SPEED BREAKERS

IN PARTIAL FULFILLMENT OF THE REQUIREMENTS
FOR
THE DEGREE OF MASTER OF SCIENCE
IN
ELECTRICAL AND ELECTRONICS ENGINEERING

BY

MANAR ALAA KHUDHUR ALOBAIDI

ÇANKIRI

2023

DESIGN OF POWER GENERATION SYSTEM USING SPEED BREAKERS

By Manar Alaa Khudhur AL-OBAIDI

August 2023

We certify that we have read this thesis and that in our opinion it is fully adequate, in scope and in quality, as a thesis for the degree of Master of Science

Advisor **:** Asst. Prof. Dr. Mustafa TEKE
Co-Advisor **:** Asst. Prof. Dr. Mehmet TÜMAY

Examining Committee Members:

Chairman **:** Asst. Prof. Dr. Zafer Civelek
Electrical and Electronics Engineering
Çankırı Karatekin University

Member **:** Asst. Prof. Dr. Mustafa TEKE
Electrical and Electronics Engineering
Çankırı Karatekin University

Member **:** Asst. Prof. Dr. Fuat TÜRK
Computer Engineering
Kırıkkale University

Approved for the Graduate School of Natural and Applied Sciences

Prof. Dr. Hamit ALYAR
Director of Graduate School

I hereby declare that all information in this document has been obtained and presented in accordance with academic rules and ethical conduct. I also declare that, as required by these rules and conduct, I have fully cited and referenced all material and results that are not original to this work.

Manar Alaa Khudhur AL-OBAIDI

ABSTRACT

DESIGN OF POWER GENERATION SYSTEM USING SPEED BREAKERS

Manar Alaa Khudhur AL-OBAIDI
Master of Science in Electrical and Electronic Engineering
Advisor: Asst. Prof. Dr. Mustafa TEKE
Co-Advisor: Asst. Prof. Dr. Mehmet TÜMAY
August 2023

The challenge of meeting the ever-increasing global demand for energy in an environmentally responsible manner is being faced by society today. The extensive consumption of energy has led to a crisis of power in recent years, making the need for optimal utilization of conventional energy sources critical. In this study, a focus is placed on the harnessing of kinetic energy dissipated when vehicles pass over speed brakes. It is demonstrated that a significant amount of electrical power can be generated and stored using a mechanical system. In the proposed system, a double-sided rack and pinion mechanism, an AC generator, and an AC-DC converter are utilized. The conversion of reciprocating motion into rotary motion is achieved through the rack and pinion mechanism. The force that a vehicle applies as it passes over the speed brake causes a downward movement of the rack, which causes the rotor of the AC generator to rotate. As a consequence, an AC voltage is generated and stored in a battery through a controlled AC-DC converter. Several advantages are offered by this system. Firstly, a potential for power generation in high-traffic urban areas is provided. The scalability of this system to numerous speed bumps and traffic-calming features in most cities suggests that a significant amount of energy could be captured. Secondly, an enhancement in energy efficiency and environmental sustainability is promoted by repurposing otherwise wasted kinetic energy. Thirdly, a practical application is realized by using the stored energy to power streetlights during nighttime, thereby reducing the load on conventional power systems. Technical challenges associated with the design, durability, and maintenance of the system are also addressed in this study. Specifications for design, materials used, and technical requirements are outlined to mitigate the constant mechanical stress inflicted by passing vehicles. Data are presented to estimate the potential amount of energy that could be captured, based on variables such as traffic flow, vehicle weight, and speed. Benefits in terms of carbon footprint reduction are also elucidated. In summary, the feasibility and benefits of harnessing otherwise wasted kinetic energy from passing vehicles for electrical power generation are demonstrated by this study. An alternative means of power generation is provided, and a step towards a more sustainable future is represented by this research. A contribution to the broader goals of energy optimization and environmental sustainability is made by transforming an ordinary traffic-calming feature into a source of renewable energy. The alignment of this system with sustainability goals showcases the potential for innovative energy solutions. The urgency of the current energy crisis and the threat of climate change make the practical applications of such an approach particularly monumental. A paradigm shift in how energy is perceived and utilized in daily life could potentially be driven by the findings of this study.

2023, 66 pages

Keywords: Speed brake, Generator, Converter, Non-conventional energy

ÖZET

HIZ KESİCİLER KULLANILARAK ENERJİ ÜRETİM SİSTEMİNİN TASARIMI

Manar Alaa Khudhur AL-OBAIDI
Elektrik ve Elektronik Mühendisliği, Yüksek Lisans
Tez Danışmanı: Dr. Öğr. Üyesi Mustafa TEKE
Ek Danışmanı: Dr. Öğr. Üyesi Mehmet TÜMAY
Ağustos 2023

Bugünkü toplum, enerji talebinin sürekli artan küresel ihtiyacını çevresel olarak sorumlu bir biçimde karşılama zorluğuyla yüz yüzedir. Enerjinin geniş ölçekli tüketimi, son yıllarda enerji krizine yol açmış, bu da geleneksel enerji kaynaklarının en uygun şekilde kullanılmasını kritik hale getirmiştir. Bu çalışmada, odak nokta, araçların hız kesiciler üzerinden geçerken dağılan kinetik enerjiyi toplama üzerinedir. Çalışmada, önemli miktarda elektrik enerjisinin bir mekanik sistem kullanarak üretilebileceği ve depolanabileceği gösterilmektedir. Önerilen sistemde, çift taraflı bir dişli ve pinyon mekanizması, bir AC jeneratörü ve bir AC-DC dönüştürücü kullanılmaktadır. Dişli ve pinyon mekanizması sayesinde, gidip gelir hareket döner harekete dönüştürülmektedir. Bir aracın hız kesici üzerinden geçerken uyguladığı kuvvet, dişlinin aşağıya doğru hareket etmesine neden olur, bu da AC jeneratörünün rotorunun dönmesini sağlar. Sonuç olarak, bir AC voltaj üretilir ve kontrol edilmiş bir AC-DC dönüştürücü aracılığıyla bir pilde depolanır. Bu sistem tarafından birçok avantaj sunulmaktadır. İlk olarak, yüksek trafikli kentsel alanlarda enerji üretme potansiyeli sağlanmaktadır. Bu sistemin birçok şehirdeki hız kesiciler ve trafik yatıştırma özelliklerine kolaylıkla ölçeklendirilebilir olması, önemli miktarda enerjinin yakalanabileceğini göstermektedir. İkinci olarak, başka türlü israf edilecek kinetik enerjinin yeniden amaçlandırılmasıyla enerji verimliliği ve çevresel sürdürülebilirlik teşvik edilmektedir. Üçüncü olarak, depolanan enerjinin gece boyunca sokak lambalarını çalıştırmak için kullanılmasıyla, geleneksel enerji sistemlerine olan yük azaltılmaktadır. Bu çalışmada, sistemin tasarımı, dayanıklılığı ve bakımı ile ilgili teknik zorluklar da ele alınmaktadır. Tasarım için özellikler, kullanılan malzemeler ve teknik gereksinimler, geçen araçlar tarafından uygulanan sürekli mekanik strese karşı koymak için belirtilmektedir. Trafik akışı, araç ağırlığı ve hız gibi değişkenlere dayalı olarak yakalanabilecek enerjinin potansiyel miktarını tahmin etmek için veriler sunulmaktadır. Karbon ayak izi azaltma açısından faydalar da açıklanmaktadır. Özetle, bu çalışma, geçen araçlardan boşa giden kinetik enerjinin elektrik enerjisi üretimi için nasıl kullanılabileceği konusunda olanakları ve faydaları göstermektedir. Alternatif bir enerji üretim yolu sağlanmış ve bu araştırma daha sürdürülebilir bir geleceğe doğru bir adımı temsil etmektedir. Sıradan bir trafik yatıştırma özelliğini yenilenebilir enerji kaynağına dönüştürerek enerji optimizasyonu ve çevresel sürdürülebilirlik gibi geniş hedeflere katkıda bulunulmuştur. Bu sistemin sürdürülebilirlik hedefleriyle uyumu, yenilikçi enerji çözümleri için potansiyeli sergilemektedir. Mevcut enerji krizinin aciliyeti ve iklim değişikliği tehdidi, böyle bir yaklaşımın pratik uygulamalarını özellikle anlamlı kılmaktadır. Bu çalışmanın bulguları, enerjinin günlük yaşamda nasıl algılandığı ve kullanıldığı konusunda potansiyel olarak bir paradigma değişikliği sürükleyebilir.

2023, 66 sayfa

Anahtar Kelimeler: Hız freni, jeneratör, konvertör, konvansiyonel olmayan enerji

PREFACE AND ACKNOWLEDGEMENTS

I would like to thank my thesis advisor, Asst. Prof. Dr. Mustafa TEKE, and co-advisor Asst. Prof. Dr. Mehmet TÜMAY for their patience, guidance and understanding.

Manar Alaa Khudhur AL-OBAIDI
Çankırı-2023

CONTENTS

LIST OF SYMBOLS

a	Area
vm	Average speed of the pitch line
σ	Charge concentration
$u(t)$	Control signal
d_p	Diameter
D	Diameter of the pitch circle
P	Diameter pitch
D	Duty cycle of switch
$e(t)$	Error
F_r	Force to rack
μ	Friction coefficient
Q_{SW}	Giant pulse formation switch
g	Gravity
x	Hypothetical amount of distance
ΔI_L	Inductor current ripple
J	Inertial polar moment
Ft	Load of the tangential tooth
m	Mass
Vm	Maximum thyristors reverse voltage
v_{max}	Maximum translational velocity
N	No. of teeth
Y_r	Number of gear teeth
Y_p	Number of pinion teeth
P	Number of poles
D_o	Outer diameter
Do	Outer diameter
n_p	Pinion maximum rotational velocity
r_p	Pinion radius
T_p	Pinion torque
Φ	Pinion-angle
F_e	Pressing force
ra	Radius addendum circle
rpm	Revolutions per minute
r	Shaft radius
τ	Stress
ωt	Time interval
T	Transmitted torque
tc	Turn-off time
Kv	Velocity factor

LIST OF ABBREVIATIONS

AC	Alternative current
DC	Direct current
RDSON	Drain source on resistance
EMF	Electric magnetic field
FET	Field effect transistor
FOM	Figure of merit
FOMOSS	Floating rate mosfet transistor
QGD	Gate charge discharged
VGS	Gate voltage source
HS-MOSFET	High current mosfet transistor
HS & LS-FET	High side and low side field effect transistor
IC	Integrated circuit
LDR	Light dependent resistor
MOSFET	Metal oxide semiconductor field effect transistor
PI	Proportional Integral
PID	Proportional integral derivative
PWM	Pulse width modulation
RLE	Resistor inductor with voltage source
RPG	Rod power generation
RMS	Root mean square
SW	Shortwave transistor
SCR	Silicon controlled rectifier
SBPG	Speed brake control generator
VDS	Voltage overshoot spike

LIST OF FIGURES

LIST OF TABLES

1. INTRODUCTION

The increasing energy demand presents a need for employing non-conventional energy resources. In this study, we will discuss the idea of energy producing from a speed brake and the mechanisms that are important for this. A crisis regarding energy is defined as any critical rise in pricing of supplying power to a certain economy. Generally, it means the lack of oil, electrical power, or any other natural energy resources. The political protests which took place during the 2007 Burmese anti-government riots were basically caused by rising power pricings.

Also, the Russia-Ukraine and Russia-Belarus gas dispute have been resolved prior to entering a long crisis. The reason behind a crisis could be due to industrial events such as union-organized strikes and government bans. The cause for that might be aging consumption, infrastructure, and/or sometimes bottlenecks at oil refineries and port facilities not to mention certain restrictions on fuel supply. A crises that may arise during unusually cold winters. The conventional old-fashion fossil fuels will be the basic resources of power, however, it is feared that these sources will eventually get exhausted in the coming few decades. This is why we need to investigate alternative and new resources for power generation, which will not be exhausted in the next few years. Additionally, there is the issue of pollution, which we all, living organisms, are suffering from whether on land, water, or in the air. Factories and cars are the main cause of pollution.

Consequently, we need to look for other sorts of renewable energy sources, which provide electrical power without the need to use any commercial fossil fuels or causing any harmful products. Such systems actually do exist now using different clean energy resources for power generation like solar energy, wind, OTEC (Ocean Thermal Energy Conversions), etc. For instance, we mention the latest technology employed to produce renewable, that is the “POWER HUMP " (Abdalla *et al.* 2021, Khan *et al.* 2022).

1.1 Motivations

Over the past years, the wide development in industry and number of population have caused a burst in the overall demand of global energy. Also, nowadays, there is a persistent world-wide need for clean and renewable energy resources. The conventional fossil-fuel based energies are not renewable and need limited natural sources that are fading due to the elevated cost and extracting methods that damage the environment. Thus, inexpensive and easily-obtained energy sources are becoming quite necessary (Dmitriev 2013). Our study tries to demonstrate the way energy could be tapped and used by means of road speed brakes. There is a huge number of automobiles passing over speed brakes. Consequently, and due to heat and friction, a large amount of energy is dissipated. This wasted energy can be tapped, converted into electricity, and eventually used for powering lights near the speed brake systems.

In this study, we attempt to manufacture a bump that benefits from the kinetic energy of cars/automobiles for producing power. This sort of bump may be best suitable in areas where the speed brake might be necessary. For example, toll bridges or car parking are the most suitable places for their utilization. Moreover, the study illustrates the drawbacks of currently used techniques and obstacles that these methods encounter.

1.2 Thesis Outlines

This thesis is meticulously structured into six comprehensive chapters. Chapter 1 provides a general introduction, laying the groundwork by setting the context and introducing the thesis's main themes. Chapter 2 delves into a thorough literature review, dissecting and analyzing the prevailing works relevant to the study. Chapter 3 presents the materials and methods, detailing the means and processes utilized to gather data and perform the study. In Chapter 4, the power calculations are meticulously explained, providing critical insights into the mathematical models and computational aspects of the study with the nano-economical analysis to the system. Following this, Chapter 5 unveils the simulation results, interpreting and presenting the outcomes derived from the study's simulations.

Finally, Chapter 6 encapsulates the conclusion, providing a thoughtful synopsis of the findings, potential implications, and recommendations for future research.

2. LITERATURE REVIEW

Road gower generation is a system designed to tap kinetic energy from all cars/automobiles moving on the road. In this method, a device is used to convert the vehicles kinetic energy into electrical power. This is carried out by fixing a moving plate on the street, it senses any tiny motion on the street surface and transfers to a flywheel system. Now, out of numerous wheels lies a single flywheel utilized to drive machinery. An Road gower generation system employs the technique of driving a single flywheel to another when it reaches a previously determined speed. It has been designed to get a relatively large amount of inertia within a small area (Sinha *et al.* 2021).

The energy can be harvested and utilized from street speed bumps with numerous vehicles passing over speed bumps daily, a substantial amount of energy is dissipated as heat and friction at these locations. This wasted energy can be harnessed and converted into power by transforming the speed bump into a power-generating unit. The energy produced in this manner can be used to illuminate the streetlights adjacent to the speed bumps (Dara *et al.* 2020)

Unlike many developed nations, India contends with poorly constructed roads. By installing a power generation unit from speed bumps adjacent to specific streetlights, a vast amount of energy could be captured and stored for later use to light both sides of the street. As a result, some of the electricity that was previously used by these lights can now be redirected to power these towns (Maurya *et al.* 2016).

The rotating part (rotor) is connected to the main motor and moves with the rotation of the main motor. The rotor has a magnet which, when rotating, creates a magnetic field. The moving part is enclosed in a fixed case (the stator) that contains a coppered coil or winding. When a magnetic field flows through the coil, electrical power is generated. A car that weighs 1000 kg and climbs 10 cm on this massive strip produces about 0.98 kW. For example, one of these high-speed locomotives on a high-traffic street, where about 100 cars go by every single minute, can produce about 1 kilowatt of electrical power per minute. This result could be remarkable at the end of the day. An inverter must be installed on each vibrating belt to capture this electrical energy (Srivastava and Asthana 2011).

It is exceptionally crucial to plan a pollution-free vitality-era framework. Speed Brake Control Generator (SBCG) is the foremost rising procedure that provides electrical control with the least input value. An exploratory ponder to create power by SBCG, where a rack and pinion instrument is utilized for generating power. Whenever a vehicle passes on the speed brake, then the rack will move to descend create direct-to-revolving movement much appreciated to the pinion. This rotational movement is exchanged to a DC generator to produce DC control, which is put away in batteries like in sun-powered innovation. The created control can be utilized for household purposes or indeed commercial offices, which are shown close to the speed brake. It turned out that this SBCG produces 273.24 Watts on one thrust when applying 400kg. So, within one hour, 100 vehicles weighted 400kg may produce 54.59 kWh. It utilizes descending as well as upward development of the rack (Azam *et al.* 2020).

Mishra *et al.* (2012) presented a system for generating electricity from a speed brake. It is designed using a double-sided rack and pinion, ac generator, and AC-DC converter to store the energy produced in a battery. Energy has continuously been an essential requirement for the survival of all life forms over the universe. Everything that takes put around us is the expression of power change from one frame to another. In any case, in this fast-moving world, the more the populace is expanding, the more the customary power sources are diminishing. The broad utilization of power all over the world has brought about at a power emergency over the past few a long time. So, to avoid this issue, we got to execute the procedures of optimum use of ordinary power sources. In this extend, we'll clarify how to utilize the power scattered when vehicles pass over a speed brake since a noteworthy sum of power is created at whatever point a vehicle passes over it.

3. MATERIALS AND METHODS

This study is to produce electrical energy out of speed brakes. The load, any moving vehicle, presses the speed brake, causing the rack&pinion mechanism to move. The translational movement of the speed brake is transformed into rotational movement thanks to the rack-pinion mechanism. The gear is coupled with the pinion axis that meshes a pinion. When the energy is transferred (gear to pinion), the velocity is relatively multiplied at the rotation of the pinion. The equip with the larger measurements is connected to the pinion hub. The pinion networks to the adapt. That is why, as the adapt moves at the duplicated pinion speed, it increases the speed to the next escalated. So, although the speed accomplished at the primary adapt has a lesser value, as the control is transferred to gears the velocity is increased to a much higher value, which velocity is adequate to turn the rotor of a generator. The rotor turning inside an inactive attractive stator intersects the flux encompassing it, hence creating the EMF which is, at that point, sent to a bridge rectifying stage, where the produced AC is changed over to DC. The EMF is utilized to charge the battery as appeared in Figure 3.1 (Dara *et al.* 2020, Kale *et al.* 2021).

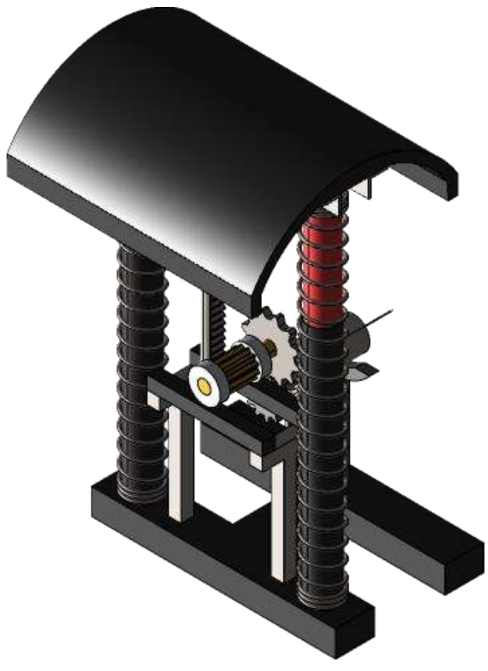

Figure 3.1 Electrical power generating mechanism (Sai 2021)

3.1 Mechanical Parts

3.1.1 Coil spring mechanism

A coil spring mechanism utilizes the potential energy stored within a tightly wound spring to perform work. Also known as helical springs, coil springs are among the most common types of springs. The mechanism consists of a wire or metal rod that is wound into a series of coils. When a force is applied to the spring, it compresses or extends, storing potential energy. When the force is removed, the spring returns to its original shape, releasing that stored energy. Figure 3.2 shows the coil spring movement (Wada and Minoru Taya 2002).

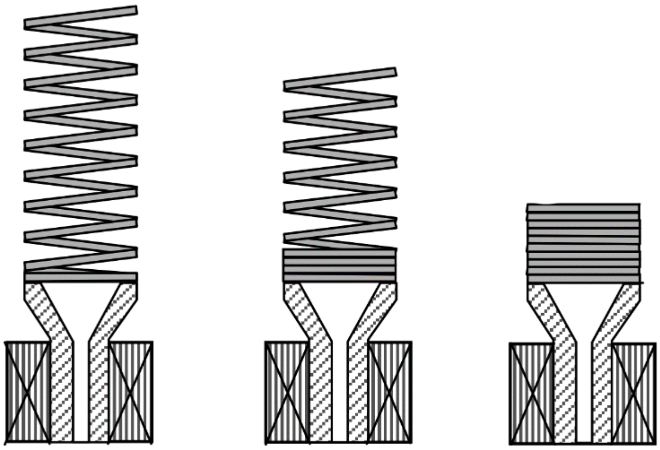

Figure 3.2 Coil spring movement (Wada and Minoru Taya 2002)

Coil springs are used in a variety of applications. Automotive suspension systems often use coil springs to absorb shocks from the road and provide a smoother ride. In a smaller scale, coil springs are used in pens, retractable cords, and even in trampolines. Large industrial machinery may also use coil springs to handle vibrations or heavy loads. There are many type of coil-spring:

1. Compression Coil Springs: This is perhaps the most common type of coil spring. When a force is applied to a compression spring, it contracts or compresses, storing mechanical energy. When that force is released, the spring expands back to its original length.

2. Extension Coil Springs: Also known as tension springs, extension coil springs do the opposite of compression springs. They store mechanical energy when they are stretched or extended, and when the force is removed, they return to their original length.
3. Torsion Coil Springs: These are designed to store mechanical energy when they are twisted. When the force causing the twist is removed, the spring rotates in the opposite direction to return to its original shape.

3.1.2 Rack pinion mechanism

A rack and pinion is a type of linear actuator that comprises a circular gear (the pinion) engaging a linear gear (the rack), converting rotational motion into linear motion (and vice versa). This system is commonly used in car steering systems, where it translates the rotation of the steering wheel into the side-to-side motion of the wheels (Yan *et al.* 2019) (Figure 3.3).

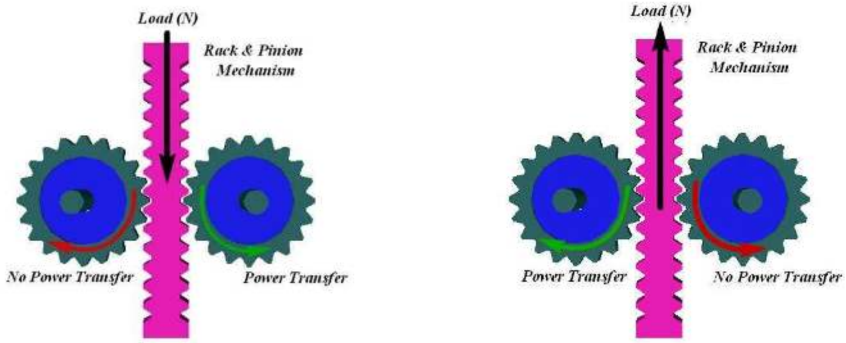

Figure 3.3 Rack-pinion mechanism (Azam *et al.* 2016)

The integration of a rack and pinion mechanism into road speed breakers can have several advantages and disadvantages. Advantages include less backlash, providing a smooth energy transfer and reducing the 'play' when reversing the direction of movement. Greater feedback is also a key advantage due to the direct connection between the rack and pinion, facilitating the immediate translation of changes in vehicle weight or speed into mechanical motion. Accurate displacement allows for precise calculations of energy generation based on vehicle weight and speed, aiding in better energy management. However, there are disadvantages, such as the requirement for more guiding supports to ensure proper alignment and durability under constant vehicular pressure. Additionally, due to the potentially high rotational speeds generated by direct contact between the rack and pinion, especially from fast or heavy vehicles, additional gear reduction systems may be needed to protect the generator and ensure optimal operation, which adds to the system's complexity and cost (Dara *et al.* 2020).

3.1.3 Crank-shaft mechanism

Implementing a crankshaft mechanism in road speed breakers involves converting the linear motion caused by vehicles passing over the speed breaker into rotational motion, potentially harnessing energy. As a vehicle traverses the speed breaker, it depresses a lever arm connected to a crankshaft. The downward force on the lever arm rotates the crankshaft, and this rotational motion can be used to drive a mechanical system or generate electricity. As the vehicle passes and the lever arm rises back, the crankshaft completes a full revolution. While this system provides an innovative approach to energy harvesting, it also demands robust construction to withstand constant vehicular stress and precise engineering to handle the balance between the downward force of various vehicles and the mechanical resistance of the system. Figure 3.4 show crank-shaft using in road speed breakers (Durai 2017).

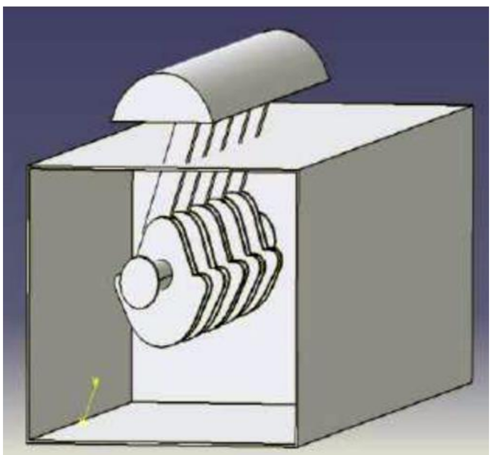

Figure 3.4 Crank-shaft using in road speed breakers (Durai 2017)

Implementing a crankshaft mechanism in road speed breakers offers certain advantages and disadvantages. On the positive side, this mechanism does not require any direct connections with the speed breaker, simplifying the installation and operation process. Additionally, maintenance is relatively easier as the mechanism's components are more accessible, reducing downtime for repairs or upgrades. However, disadvantages include a heavier construction, resulting from the robustness required to withstand vehicular stress, which can complicate the installation process and increase costs. Moreover, the mechanism occupies more space due to its design, demanding more room beneath the speed breaker, which may not always be available or may necessitate additional roadwork for proper installation.

3.1.4 Chain sprocket

The chain sprocket utilized basically changes over the input direct movement into a rotational movement to the rotor shaft. The shaft acts as an input to the DC power generator that produces the specified electrical field. Chain-sprocket is valuable whenever the remove among shafts is quite large when compared to the required equip estimate. This is why a bicycle employment a chain-sprocket is that the required remove among the two shafts is badly designed for gear-2-gear fitting. Of course, you may consider a drive shaft like in a vehicle but that may by be heavier, more troublesome to bundle, and less strong. Clearly, when it comes to bikes, the lighter the superior. Therefore, in brief, chain-sprocket is the lightest transmission conceivable that could convey the toughness requested by buyers. Bikes that utilize shaft drivers, a sort of rack-pinion adapt instrument, have as well numerous impediments for standard adoption.

In any case, they have held on in specialty markets for over a hundred a long time, for the most part through oddity offer. For occasion, the Sonoma D-drive appeared underneath is offered at Walmart as a commuter bicycle. Shaft drivers couldn't be as popular as chain-and-sprocket plans for a few reasons such as weight, higher fetched, included complexity, troublesome upkeep, and low-value mechanical proficiency. The problem is that each issue illuminated by a shaft driver can too be illuminated with a chain case, but for the truth that it is impossible to see cool whereas riding a bicycle with a chain case.

Furthermore, shaft & gears must be moderately little and quite solid because of the extraordinary rotating drive. As a result, they are heavier and more expensive than the chain drivers. The outline has got to be more grounded as well, which suggests indeed more weight and higher cost. (Ji *et al.* 2021, Minaev *et al.* 2021, Padma Rao *et al.* 2014, Fawade 2015).

Figure 3.5 shows the chain and the sprocket. Later in the simulation, this part is modeled as a simple gain block.

Figure 3.5 Chain and sprocket

3.1.5 Roller mechanism

A roller mechanism incorporated into road speed breakers is another innovative method of energy recovery. This system involves a set of rollers embedded within the speed breaker. As a vehicle passes over the speed breaker, its weight causes the rollers to turn. The rotational motion of the rollers can be connected, through a system of gears, to a generator that produces electricity. This is a relatively simple and straightforward method of energy harvesting, transforming the kinetic energy of passing vehicles into electrical power. This system, in essence, acts as a miniaturized and decentralized power generation unit, taking advantage of the energy otherwise lost in slowing down vehicles at speed breakers. Similar to other mechanisms, this approach also requires careful engineering to ensure durability under repeated vehicular stress and to optimize energy generation efficiency. Figure 3.6 shows the roller unit mechanism.

Figure 3.6 Roller unit (Padma Rao *et al.* 2014)

Implementing a roller mechanism in road speed breakers presents both advantages and disadvantages. A notable advantage is the relative ease of construction, which also contributes to its lower cost, making it a viable option for areas with budget constraints. However, this system tends to be less effective in energy conversion compared to other mechanisms, primarily due to the potential for slippage between the rollers and vehicle tires, leading to less efficient energy capture (Ahmed *et al.* 2020, Dara *et al.* 2020, Bintu *et al.* 2022, Sinha *et al.* 2021, Kushwaha *et al.* 2020, Naveen *et al.* 2022).

Whenever a car moves over a speed brake, it moves downward with a distance (x) cm. While, the rack simultaneously moves downward in the same distance (x) cm. Both the rack and pinion are meshed together, which is connected to the gear shaft. The gear with (yr) teeth meshes with the pinion that has (yp) teeth, which in turn is coupled along with the motor generator. This mechanism transforms translational movement into rotary movement. When the shaft of the generator turns, it produces a current that is proportional to the No. pinion turns. The current generated is then stored inside a battery. Afterwards, the rack is moved back to its original position by means of a spring mechanism.

3.2 Tangential Force on the Rack - Maximum Rotational Speed of the Pinion

When considering a horizontal application, two forces are applied to the rack because of the mass movement: Firstly, a force acting against the guide rails friction coefficient. Secondly, a force resulting from mass acceleration. Not to mention that, if any external pressing forces are present, they will be implied in the tangential force. Equation (3.1) represented to the applied foruce to rack.

$$F_r = mg\mu + maF_e \tag{3.1}$$

Where : F_r Force applied to rack, m moving mass, g gravity, μ friction coefficient. (Between 0.002 to 0.003 for the ball/roller guides), F_e pressing force, if applied.

Now in a vertical motion, the load moves in the guide system direction. Thus, the force of the moving mass will not be subject to the friction of the guide rails. (Xu *et al.* 2020, Antipin *et al.* 2022).

Equation (2.2) represented to applied force to the rack

$$F_r = mg + ma + F_e \tag{3.2}$$

The pinion torque is merely the tangential force multiplied by the radius of the pinion as shown in Figure 3.7. Also in Equation (3.3) and Equation (3.4).

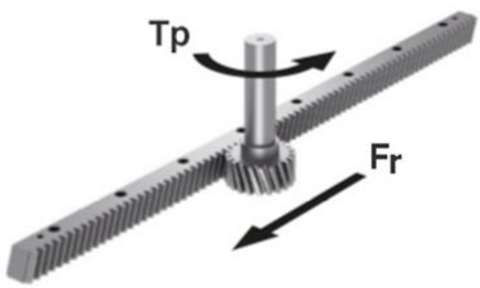

Figure 3.7 Pinion torque

$$T_p = F_r r_p \tag{3.3}$$

$$r_p = d_p/2000 \tag{3.4}$$

Where: T_p Pinion torque, r_p Pinion radius and d_p Diameter.

The maximal rotational velocity of the pinion. In order to identify the maximal pinion angular velocity, we divide the maximal translational velocity as in Equetion (3.5)

$$\pi * d_p \tag{3.5}$$

Also, Units must be convertted from mm to m, and from m/s to rpm.

Also, pinion maximum rotational velocity Equation (3.6)

$$n_p = \frac{v_{max} 60 * 1000}{\pi d_p} \tag{3.6}$$

Where: n_p is the pinion maximum rotational velocity and v_{max} is the maximum translational velocity.

3.3 AC Generator

Essentially, an Alternating Current (AC) generator is an electrical machine that changes over mechanical power into electrical within the shape of an AC. The essential guideline of the working principle of an AC machine is Faraday's law of electrical acceptance, to some degree comparable to the behavior of a DC generator as shown in Figure 3.8 which outlines the way an AC synchronous generator functions.

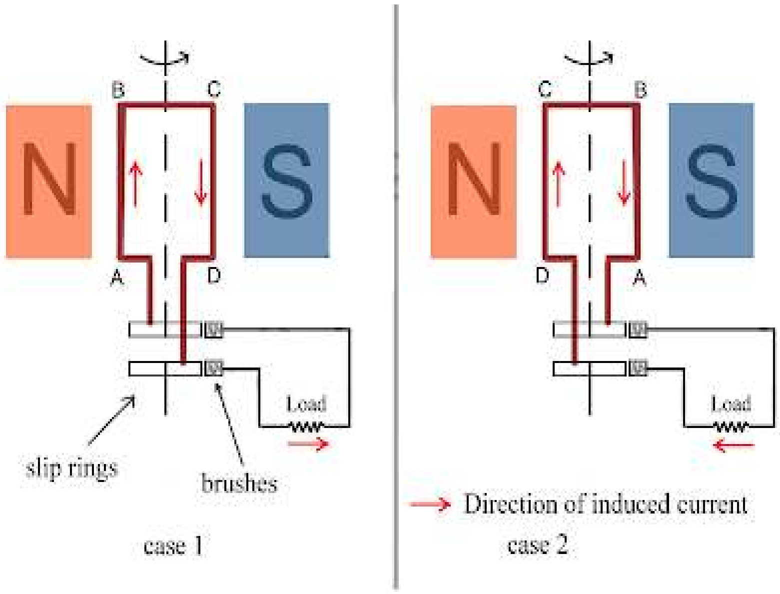

Figure 3.8 AC Synchronous generator

Agreeing to Faraday's law, at whatever point a conductor displaces in a magnetic field, EMF is actuated over the conductor. On the off chance that a closed loop is given to the conductor, actuated EMF causes current to stream within the circuit.

If the winding A-B-C-D is placed in a magnetic field. The heading of the flux is from the N to S. The winding is associated to slip rings, and the stack is associated through brushes fixed on the slip rings. The winding is pivoting clockwise so the heading of the actuated current is given by the right-hand law.

When pivoting clockwise, the winding position changes after half of the rotational period. The heading of the actuated current, concurring to the right-hand law, is in the direction D-C-B-A. This appears that the heading of the current alters after each half of the rotational cycle, which implies we achieve an AC current. (Zhang and Wei 2020, Kučera *et al.* 2020, Li and Wang 2022). The most parts of an alternator are the stator and rotor. However, not at all like other machines, in most of the AC machines, it is the field exciters that pivot whereas the armature coil remains stationary as outlined in Figure 3.9.

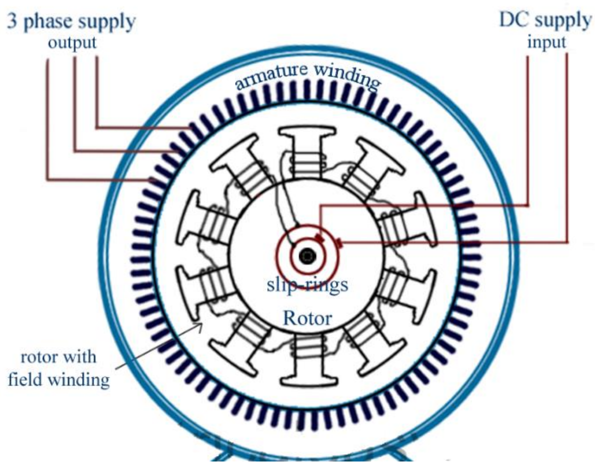

Figure 3.9 Salient pole type alternator AC stator

Not at all like in a DC machine, isn't the alternator stator suggested to provide a way for the magnetic flux. To determine EMF Equation (3.7) and Equation (3.8) let us consider the following symbols:

$$\text{EMF (t)} = -\frac{d\phi}{dt} = -N' - \frac{d\phi}{dt} \tag{3.7}$$

$$\phi = \phi_m \sin\ \omega t \tag{3.8}$$

Instantaneous EMF after neglecting the direction consideration could be written as Equation (3.9), (3.10), (3.11) and (3.12).

$$e = N' \frac{d}{dt}(\phi_m \sin\ \omega t) \tag{3.9}$$

$$e = \frac{Z'}{2}\omega\phi_m \cos\ \omega t \tag{3.10}$$

$$e = \frac{Z'}{2}\omega\Phi\cos\ \alpha: \tag{3.11}$$

$$\Phi = \phi_m; \alpha = \omega t \tag{3.12}$$

Where: N' is the number of turns in each pole $\frac{Z'}{2}$, ϕ phase angle, Z' Number of coils per pole (Z/P) and e = Electromagnetic Field (in Volts).

The RMS voltage value calculted using Equations (3.13), (3.14) and (3.15).

$$E' = \frac{Z'}{2}\omega\Phi\left[\frac{1}{\pi}\int_{-\pi/2}^{\pi/2} \cos^2\ \alpha d\alpha\right]^{1/2} \tag{3.13}$$

$$E' = \frac{Z'}{2}\omega\Phi\left[\frac{1}{\pi}\int_{-\pi/2}^{\pi/2} (1+\cos\ 2\alpha) d\alpha\right]^{//2} \tag{3.14}$$

$$E' = 2.93 f Z'\Phi \tag{3.15}$$

Therefore, Z_{ph} conductors in series per phase will induce EMF Equation (3.16)

$$E_{ph} = 2.22 f Z_{ph}\Phi \tag{3.16}$$

Let Nph is the No. of turns in each phase, then Equation (3.17) be :

$$E_{ph} = 4.44 f N_{ph}\Phi \tag{3.17}$$

Also, the value of f calculated by having known the rpm and number of poles.

3.4 AC-DC Converter

A Single-Phase full converter transforms an AC to DC using only thyristors. The use of thyristors only facilitates the control of the conversion process and allows wider control over the DC voltage level.

3.4.1 RLE load one-phase full converter

It has 4 SCRs or thyristors loaded with RLE. Where R is a resistor. L is an inductor. And E is the back EMF. The EMF comes either from the presence of a battery as a load or a DC motor. Herby, the operation of a one-phase full bridge converter is presented with the circuit schematic, waveforms, output signals (RMS), and the average voltages across the RLE and R loads, respectively. Figure 3.10 illustrates a circuit of a RLE one-phase full bridge. The SCRs are T1, T2, T3, and T4.

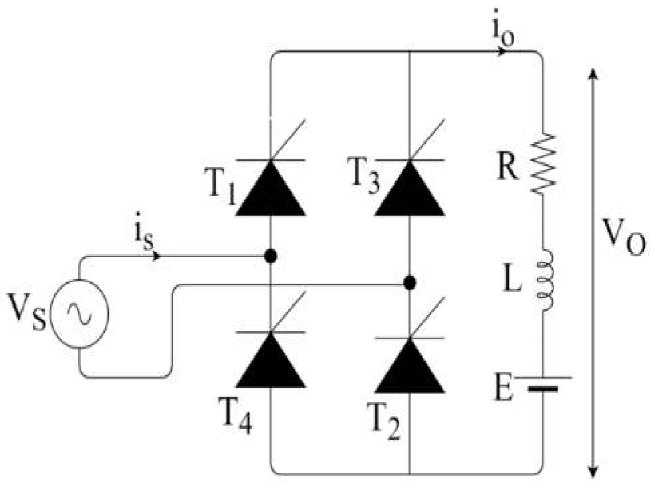

Figure 3.10 One-phase RLE full bridge converter

Every thyristor pair is triggered on at the same time. T1 & T2 are triggered at the same time and after an interval of π radian, T3 & T4 are triggered. (Chibante and Carvalho 2022, Das *et al.* 2020).

Form the time interval ωt = 0 and ωt = α. times between T1 and T2 are forward biased. Also, From the time interval between α to π+α At α, T1 & T2 are triggered on and forward biased, thus T1 and T2 start conducting. When T1 & T2 go into conduction. A voltage Vm sin α appears across T3 and T4 as a reversed biased voltage. Hence, T3 and T4 are turned off. The load current flows from T3 T4 to T1&T2. The thyristor T1and T2 which are triggered after α get turned on when Vm sin α > E. Here, T1 and T2 conduct for π radian of time i.e. from α to π+α. In the time interval between π+α to 2π+α. At (π+α), T3

& T4 are triggered. T1 and T2 are turned off. Likewise, i-o flows from T1T2 to T3 T4 and T3 T4 conducts for π radian of time i.e. from between π+α to 2π+α.

Figure 3.11 presents the waveforms of a RLE one-phase full converter - the load current Io is DC.Also, In the interval 0 to α, VS is positive. Whereas the supply current is negative as the power is negative. This means that an amount of energy from the load returns to the source. In time α to π, (Vs) and (Is) are positive (Ionta 2022).

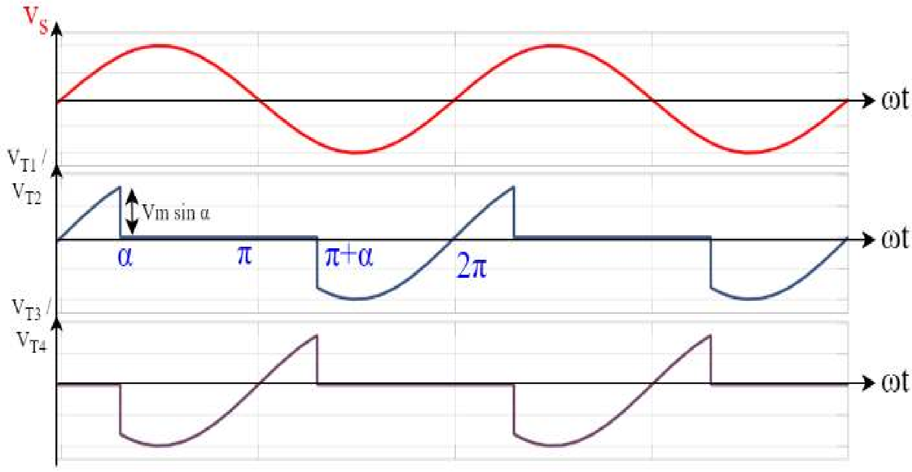

Figure 3.11 Waveforms of a RLE one-phase full bridge converter

The average output voltage V o is given by observing the waveform of output voltage Vo. Likewise, the RMS of the output voltage is given by Equations (3.18), (3.19), (3.20) and (3.21).

$$V_{ormv}^2 = \frac{1}{\pi}\int_{\alpha}^{\pi+\alpha} V_m^2 \sin^2\ \omega t d\omega t \tag{3.18}$$

$$V_{orms}^2 = \frac{V_m^2}{2\pi}[\omega t - 0.5\sin\ 2\omega t]_{\alpha}^{\pi+\alpha} \tag{3.19}$$

$$V_{armv}^2 = \frac{V_m^2}{2\pi} \tag{3.20}$$

$$V_{ornc} = V_s \tag{3.21}$$

For the one-phase full bridge converter, the turn-off time t_c is given by Equation (3.22).

$$t_c = \frac{\pi-\alpha}{\omega}\,\text{sec} \tag{3.22}$$

3.4.2 R load single phase full bridge converter

Figure 3.12 presents the circuit diagram of an R-loaded one-phase full bridge converter.

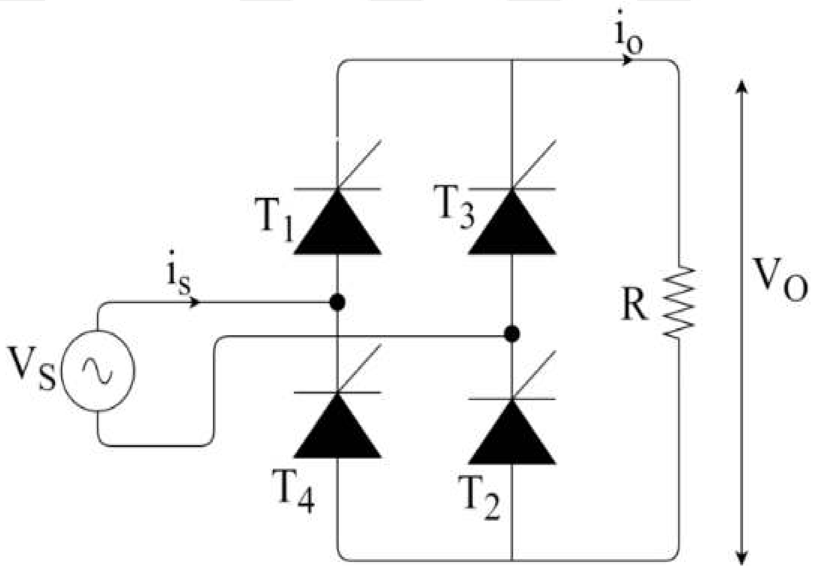

Figure 3.12 R load - one-phase full bridge converter

The thyristor T1 and T2 are on at α and conduct till π. And after π, the supply voltages are reversed and T1 & T2 are off. At instant π+α, T3 and T4 conduct to 2π.

Also, Figure 3.13 illustrates the waveforms for R-load only.

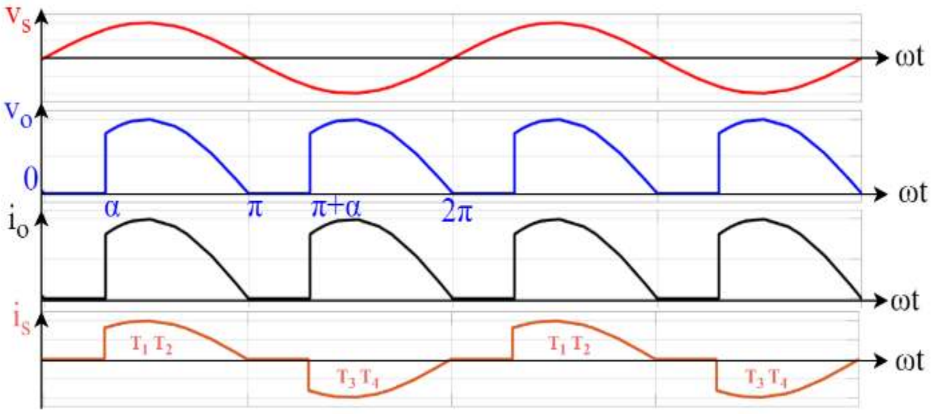

Figure 3.13 Waveforms of an R load single-phase full bridge

The output voltage average V_o is given by Equation (3.23) and Equation (3.24)

$$V_o = \frac{1}{\pi}\int_{\alpha}^{\pi} V_m \sin\ \omega t d\omega t \tag{3.23}$$

$$V_o = \frac{V_m\sqrt{2}}{\pi}(1 + \cos\ \alpha) \tag{3.24}$$

3.4.3 Buck converter

The buck converter is the foremost prevalent topology utilized to disseminate control in complex systems. It gives the specified nearby voltage from the next voltage transport that's to numerous regulators within the framework. The regulator comprises of 1 dynamic switch driven by an IC, a rectifier, and channel components. This extraordinary straightforwardness permits for low cost and higher efficiency control dispersion all through the application. The buck converter has an inductor (low pass channel) on the yield, which gives a smooth persistent yield current waveform to the stack. This may be considered a subjective advantage but it requires uncommon contemplations for enormous stack transient state. The input is uncovered to the transistor (SW). Hence, the in-current may be a exceedingly energetic wave-form, which is undesired as the exchanged current radiates clamor into the whole framework. So, to overcome this issue, an appropriate decoupling is unavoidable. (Liu *et al.* 2020)

The taking after four parameters are required to calculate the control stage where are Input voltage extend $V_{in(min)}$ and $V_{in(max)}$ also the Nominal voltage V_{out} and maximum yield current I_{out}. An IC is utilized to construct the buck converter. Usually vital since a few parameters for the calculations must be determined from the information sheet. If these parameters are known, the control organize can be effortlessly calculated. Figure 3.14 shown the buck converter circuit model.

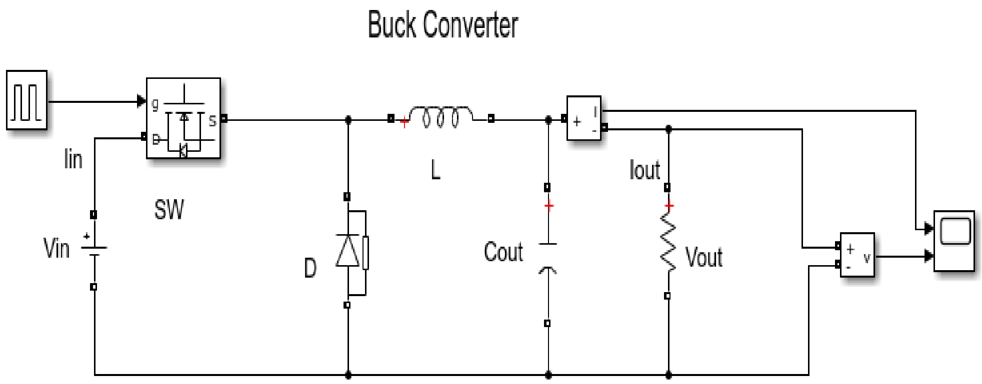

Figure 3.14 The dc-dc buck converter model

Table 3.1 presented the parameters of dc-dc buck converter which have been calculated.

Table 3.1 The dc-dc buck regulator electrical specifications

Input voltage	29V
Out voltage	24V
Switching frequency	5KHz
Inductor current ripple	$0.1{*}I_o = 0.734$
Inductance L	1.9mH
Output rated power	10W
Maximum power	220W
Voltage ripple	<20mV

- Filter inductance (L)

L value and the maximum current value are calculated depending on the per-specified maximum L current ripple. Figure 3.15 filter inductor and its signals

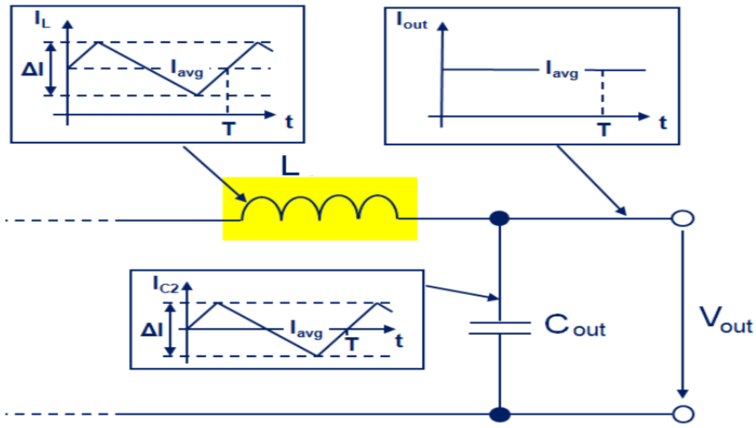

Figure 3.15 Filter inductor and its signals

Equation (3.25) and Equation (3.26) used to calculate the value of inductor voltage and inductor.

$$V_L = L\frac{di_L}{dt} = L\frac{\Delta I_L}{(1-D)T}V_{\mathrm{out}} \tag{3.25}$$

$$L = \frac{V_{\mathrm{out}}\,(V_{\mathrm{in}} - V_{\mathrm{out}}\,)}{V_{\mathrm{in}}\, f_{sw}\Delta I_L} \tag{3.26}$$

The variation in duty cycle in high-efficiency transforms doesn't have a big effect on the inductor value and may be neglected. The inductor peak current in Equation (3.27) and (3.28)

$$I_{pk} = I_{\mathrm{out}} + \frac{\Delta I_L}{2} \tag{3.27}$$

$$I_{pk} = I_{\mathrm{out}} + \frac{0.1 * I_{\mathrm{out}}}{2} = 1.05 I_{\mathrm{out}} = 1.05 * 7.3445 = 7.711\mathrm{A} \tag{3.28}$$

The inductance must keep a current peak of 7.711A without reaching saturation. Besides, it is significant that the L keeps its value at higher operating temperatures. This includes the board T and the L loss including of core loss and DCR loss.

- Rectifier Diode

The forward conduction power losses shwon in Equation (3.29).

$$P_{VFD} = V_{FD}I_{out}(1 - D) = 0.7 * 7.3448 * (1 - 0.414) = 3.01W \quad (3.29)$$

The invert recuperation misfortune is difficult to decide from the datasheet because it depends on different components. Be that as it may, when utilizing state-of-the-art exchanging MOSFETs, this misfortune is little and usually plays no part within the right selection of the transistor. These MOSFETs have got a certain advantage on switch recuperation misfortune at the value of RDSON. The dead-time misfortune is straightforwardly corresponding to the exchanging frequency, Equation (3.30) presented the power at dead time.

$$P_{\mathrm{tdead}} = V_{\mathrm{FSYnc}} I_{\mathrm{out}} (t_{\mathrm{deadH}} + t_{\mathrm{deadLL}}) f_{\mathrm{sw}} \quad (3.30)$$

A chopping frequency of 5 kHz and a dead-time for every transition equals 10 sn. As shown in Equation (3.31)

$$P_{\mathrm{treacl}} = 0.8 * (7.3448 * (10ns + 10ns)5kHz) = 0.6\mathrm{mW} \quad (3.31)$$

The driving voltage VGS (Gate-Source voltage) is also a crucial operational factor. It affects the RDS_{ON} and the chopping frequency of the transistor. In a given technology, the gate capacitor charge and its RDS_{ON} are reversely proportional. Thus, an optimum FET relies on the selected chopping frequency and gate-drive voltage.

- MOSFET

Switching MOSFET should be similar to an ideal switch (low resistance and fast chopping frequency).

In the buck converter, the MOSFET is chosen as follows:

- QGD/QGS<1, dv/dt actuated turn-on.
- High switching frequency switch (on/off).
- Power loss due to switching must be adjusted for higher efficiency.
- Handling VDS spikes (voltage overshoot).
- Low thermal resistance RthJC.
- Diode speed and switch recuperation charge are not vital.

The Equations (3.32), (3.33), (3.34), (3.35) and (3.38) for Power losses in MOSFETs.

$$P_{HScond} = I_{\text{out}}^2 R_{D_{SON\_HS}} * D = 53.94 * 5\text{m}\Omega^*(0.1) = 27\text{mW} \tag{3.32}$$

Output capacitance is considered important parasitic parameters of the MOSFET. The output charge related to FOMOSS is used to measure the effect of energetic execution among diverse advances. The output MOSFET capacitor is charged when the HS-FET is off and broke down (scattered inside the channel).

$$P_{OSS\_HS} = 0.5 * Q_{OSS}HS * V_{IN} * f_{sw} = 0.5 * 6.4uS * 29 * 5\text{kHz} = 0.464\text{W} \tag{3.33}$$

Inductance switching losses (fast switching)

$$P_{SWHS} = 0.5^* L_{Strav} I_{out}^2 f_{sw} \tag{3.34}$$

The resistive switching losses (slow switching)

$$P_{SW\_HS} = V_{\text{in}}\, I_{\text{out}}\, \frac{Q_{SW}}{V_{GS}} R_{\text{Gate}}\, f_{sw} \tag{3.35}$$

With Q_{SW} being the switching charge, or the charge that must be included to permit the move of the MOSFET from the limit voltage (VDS) within the gate charge. The whole resistance within the gate drive way and VGS is the drive voltage. This condition is fair a 1st guess as the drive voltage changes amid the move.

In order to achieve good productivity, the HS-MOSFET ought to have a low FOM to supply a moo RDSON whereas exchanging quicker than I moves among HS & LS-FET inside its commutative circle. Other than, the driver has to give adequately moo drain & source resistances to drive the FET rapidly.

FETs transistors come in a broad variety of packages but when selecting such a component, keep in mind the following aspects:

- Required RDSON specifies minimum size of the package.
- Fast chopping only in low-inductive packages.
- Package resistance must be low.
- Thermal resistance should be small enough.

The desired thermal resistance R_{thJA} given in Equation (3.36).

$$R_{thJA} = \frac{T_J - T_A}{P_{\mathrm{MOSFET}}} \qquad \text{or} \qquad R_{thJA} = R_{thJC} + R_{thCA} \tag{3.36}$$

- Derivation of transfer functions for a buck converter

The transfer function to be derived is $\frac{\Delta V_{out}}{\Delta D}$ .Transfer functions are derived in two steps (Abdelmalek *et al.* 2020). First, keep in mind the Table states of the system and then determine change amounts for disturbances.

1. The coil current does not change over one period given by Equation (3.37).

$$I_L = \frac{V_{IN} - V_{out}}{sL} D + \frac{-V_{out}}{sL}(1 - D) \tag{3.37}$$

2. The capacitor charge amount does not change over one period given by Equation (3.38).

$$sCV_{out} = I_L - \frac{V_{out}}{R} \tag{3.38}$$

Determining the change amounts for an external disturbance and describe the transfer function in Equations (3.39), (3.40), (3.41), (3.42) and (3.43).

$$I_L = \frac{V_{IN} - V_{out}}{sL} D + \frac{-V_{out}}{sL}(1 - D) \tag{3.39}$$

$$I_L = sCV_{out} + \frac{V_{out}}{R} \tag{3.40}$$

$$I_L \to \underline{I_L} + \Delta i_L, V_{out} \to \underline{V_{out}} + \Delta v_{out} \tag{3.41}$$

$$sL\Delta i_L = V_{IN}\Delta D - \Delta v_{out} \tag{3.42}$$

$$sC\Delta v_{out} = \Delta i_L - \frac{\Delta v_{out}}{R} \tag{3.43}$$

Taking the previous equations to be a system of simultaneous equations and solving for $\frac{\Delta V_{out}}{\Delta D}$, we obtain the following in Equation (3.44)

$$\frac{\Delta V_{out}}{\Delta D V_{IN}} = \frac{1/LC}{s^2 + \frac{1}{RC}s + \frac{1}{LC}} \tag{3.44}$$

3.5 Techno-Economic Analysis

The establishment of energy access globally is a crucial area of focus in policy-making, since it is closely intertwined with the concepts of economic development and environmental sustainability. The ongoing energy crisis is impeding the continents' capacity to undergo economic change. The urgent necessity to address the energy crisis has presented a significant challenge, necessitating the exploration and use of alternate energy sources. To analysis of the power generating capacity, we use the techno-economic analysis of the system. Techno-economic analysis is a methodology employed to evaluate the economic worth of a particular system, hence providing guidance for investment and resource allocation decisions. The evaluation of energy systems often relies on many economic criteria, such as the Levelized Cost of Energy (LCOE), Payback period, and the power output of the system. This applies to an economic evaluation that calculates the present value of the unit cost of energy, expressed in money per kilowatt-hour. The term "it" refers to the concept that represents the ratio between the total energy generated throughout an individual's lifetime and the total expenses accrued during the same timeframe (Baribuma *et al.* 2023).

A. Power generating capacity

The mechanism produces power as each car traverses the speed bump. The power generation capacity of the system is determined by estimating the power output of the system and considering the actual traffic flow conditions. Hence, the power generating capacity (P_g) of the system may be determined using the Equation (3.45):

$$Pg = Pveh \times Q \times t \tag{3.45}$$

where P_{veh} represents the average power generated per vehicle travelling on the main supply bus (W), Q denotes the traffic flow (veh/h), and t signifies the survey period (h) (Baribuma *et al.* 2023).

B. Energy harvesting

Energy harvesting refers to the process of capturing and converting modest quantities of conveniently accessible energy from the surrounding environment into a useful form of energy, such as electricity. The energy extracted from a system is quantified using the concept of net capacity factor, which serves as an indicator of the effectiveness of energy conversion devices. The energy transducers utilized in the system design comprise a battery, buck converter, and AC to DC converter. The capacity factor (C) is determined using the Equation (3.46).

$$C = \eta bc \times \eta c \times \eta b \tag{3.46}$$

where η_{bc} represents the efficiency of the buck converter, ηc represents the efficiency of the converter, and ηb represents the battery charge efficiency.

C. Levelized cost of energy (LCOE)

The Levelized Cost of Electricity (LCOE) is a financial evaluation that determines the net present value of the cost of producing one unit of energy, expressed in currency per kilowatt-hour. The concept of the ratio between the total expenditures incurred over the lifespan of a power generation system and the amount of power generated by that system during its operational lifetime. The components that contribute to the overall cost over the lifespan of a system encompass the whole installation expenses, fuel expenditures, as well as operational and maintenance costs. The system does not require any fuel or incur running costs, and its maintenance costs are minimal.

The Levelized Cost of Electricity (LCOE) is determined by applying a Equation (3.47) to the projected operational lifespan of a power producing plant.

$$LCOE = \sum_{t=1}^{n} \frac{(It+Mt+Ft)/(1+r)^t}{Et/(1+r)^t} \tag{3.47}$$

In the given equation, the variables represent the following: I_t denotes the investment cost in year t (in USD dollors), M_t represents the operation and maintenance costs in year t (in us dollors), F_t represents the fuel cost in year t (in USD dollors), Et represents the energy generated in year t (in kilowatt-hours), r represents the discount rate (expressed as a percentage), and n is the estimated lifetime of the system (in years).

D. Payback period

The payback period is a metric used to calculate the duration, in years, required for the energy savings generated by a renewable energy system to equal or surpass the initial investment cost. The calculation of payback is determined by employing a certain Equation (3.48).

$$Yp = \frac{It}{E \times C - M} \tag{3.48}$$

In this equation, Y_p represents the payback period in years, E denotes the annual energy generation in kilowatt-hours per year (kWh/year), C represents the unit cost of energy in dollars per kilowatt-hour ($/kWh), and M represents the annual operations and maintenance cost in dollars per year ($/year). The mean cost of grid power in Iraq is $0.015 per kilowatt-hour (kWh).

E. Cost associated with the installation process

Traditionally, the expenses associated with the installation of rack and pinion were categorized into two components: the costs related to the production and installation of the main support bracket (MSB), and the costs associated with the essential supplementary components (ESS). The latter encompasses expenses for batteries, inverters, charge controllers, and installation hardware.

4. SIMULATION AND RESULTS

Models in MATLAB-SIMULINK use signal connections, which specify the way data flows among blocks. The Simscape model utilizes physical connections that allow a bidirectional energy flow among elements. One can add other stages to the mass-spring-damper by performing simple copy and paste operations. Input and/or output connections need deriving and implementing equations. Presented in this chapter are the modeling and simulation for all the system elements.

The considered system includes the following elements:

- Mass spring
- AC generator
- AC/DC converter
- Buck converter

As shown in Figure 4.1 the full system simulation.

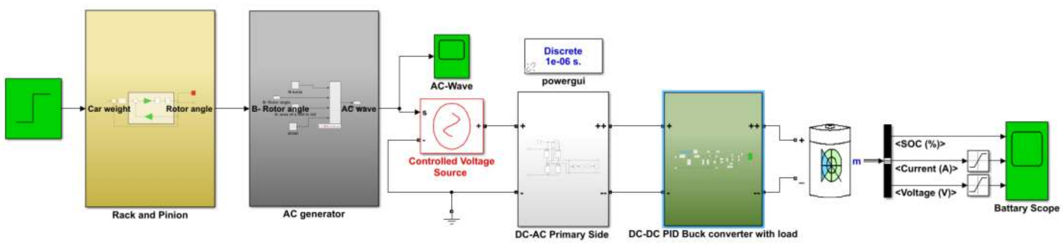

Figure 4.1 Full system model

In this chapter, we'll simulate both of the system's possible states—one with the load (whenever there is a connection made between a street light and the system) and one without it in which the battery is simply charging and there is no dynamic external effect from loads such as lighting, lighting signs, traffic signals, and other applications —and observe what happens to the system in each.

4.1 Mass Spring

Let the initial value of the deflection for the spring is 0.2 m as specified in Figure 4.2 the block annotations for the spring. The integrator blocks have a value of 1 as representive of the Equation (4.1).

$$m\ddot{x} + c\dot{x} + kx = f(t) \tag{4.1}$$

Where m is the mass, c is the damper (neglected), and k is the stiffness.

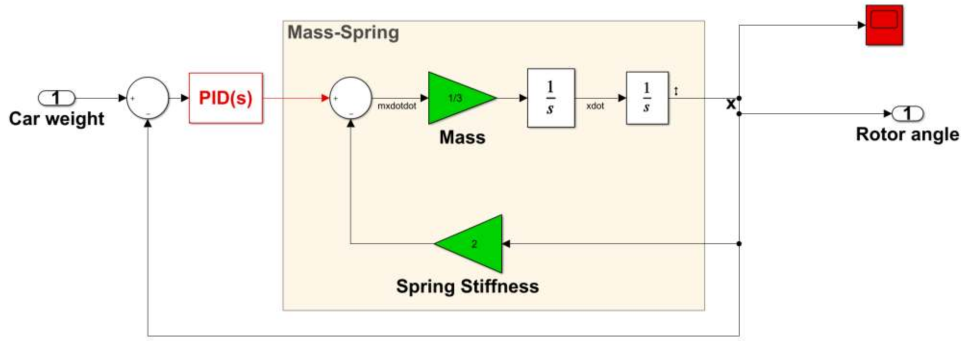

Figure 4.2 Rack and pinion model in MATLAB

Figure 4.3 presents a designed conversational interface to specify the values of the buck parameters (mass and stiffness modulus).

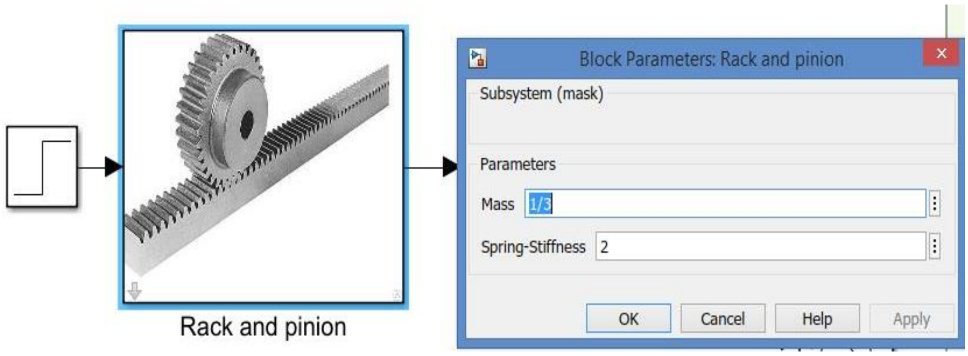

Figure 4.3 Define system parameters

Figure 4.4 shows the step response with an overshooting of less than 14% after the calibration of the traditional controller parameters. The PID controller is a corrector in the system that increases the rotor angle and achieves optimal performance if the car's weight exceeds the system's value. PID controller parameters: Proportional (P) is 204.9, integral (I) is 140.9 and derivative (D) is 63.9.

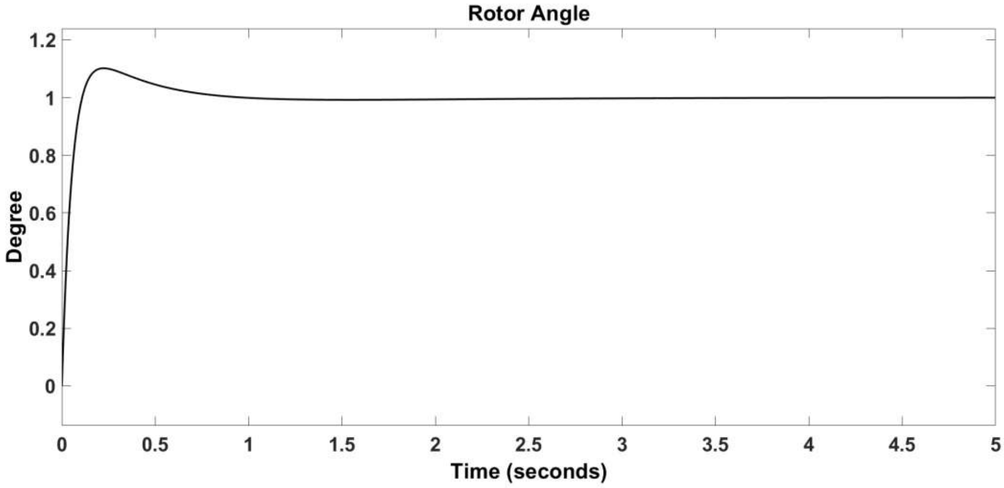

Figure 4.4 Closed-loop response of mass spring

4.2 AC Generator

It consists of a rectangular-shaped winding with 'N' turns and an 'A' area (m^2). The angular velocity 'ω', and the magnetic flux is perpendicular to the winding plane and is symbolized by B and given by (Cos ωt). The AC wave is given in Equation (4.2).

$$\varepsilon = \mathrm{NBA}\omega\sin\ \omega\mathrm{t}. \quad (4.2)$$

Figure 4.5 shows the AC enerator model in MATLAB.

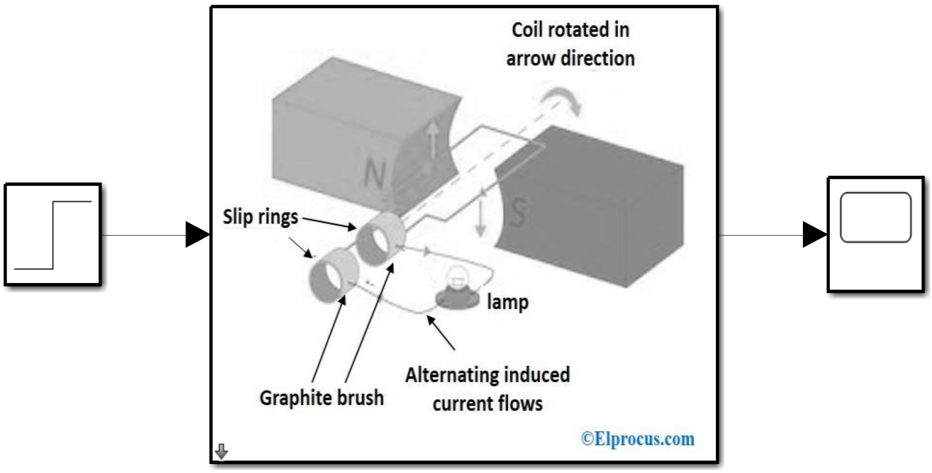

Figure 4.5 AC generator model

Figure 4.6 illustrates an interface to specify the parameters for the AC generator

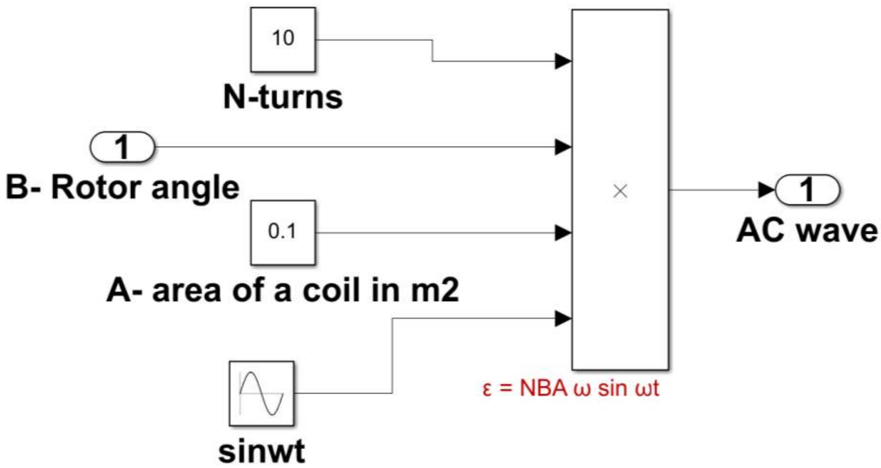

Figure 4.6 AC generator parameters

Figure 4.7 illustrates an AC generator wave

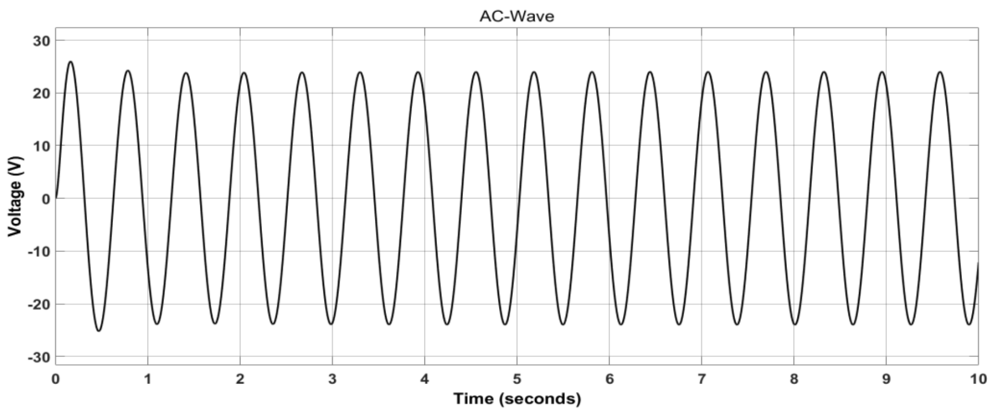

Figure 4.7 AC generator wave

4.3 AC-DC Converter

After the alternating voltage is obtained from the generator, it is converted into a suiTable constant voltage to charge the battery. Figure 4.8 shows the converter model that consists of a complete rectifier bridge and specified control signals of the transistors to ensure that it works in alternating pairs.

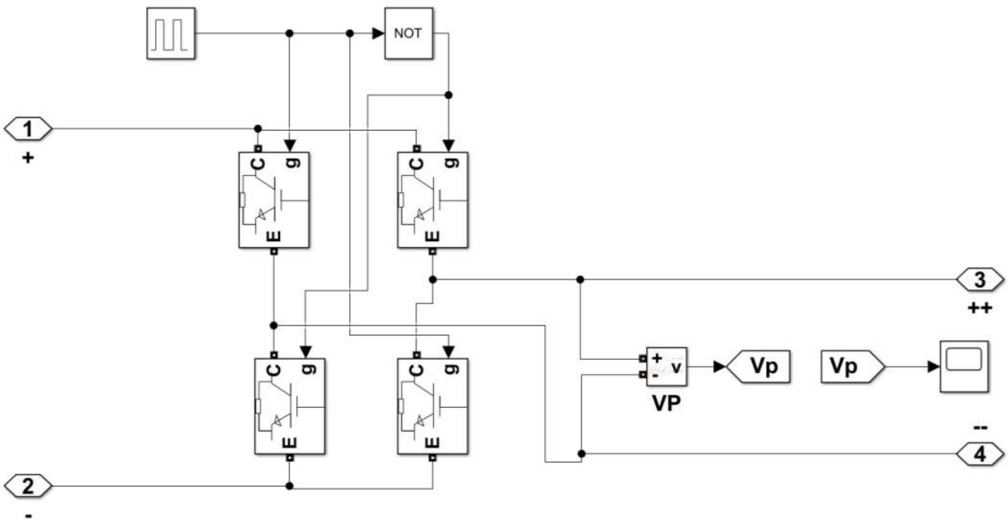

Figure 4.8 AC-DC converter

Figure 4.9 shows the control signals of the transistors.

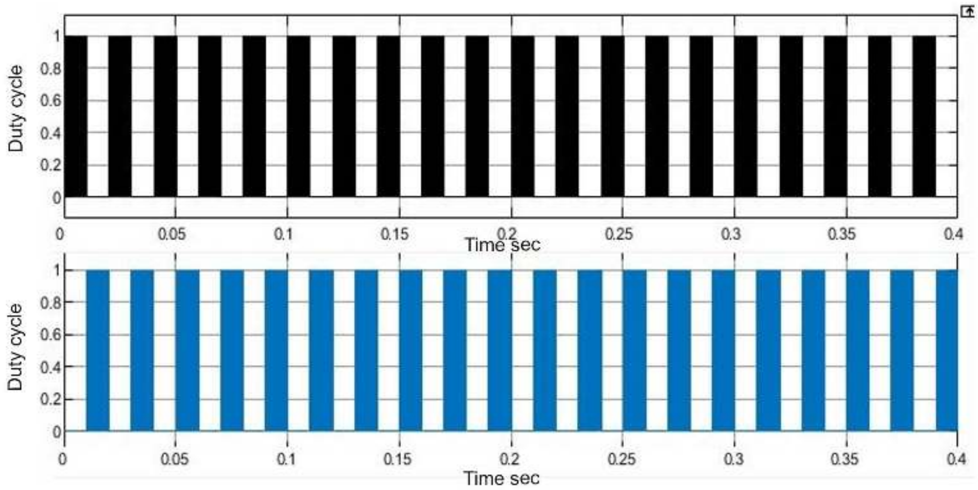

Figure 4.9 The transistors control signal

Figure 4.10 shows that the direct voltage generated by the conversion process is affected by the vibrations close to the required value.

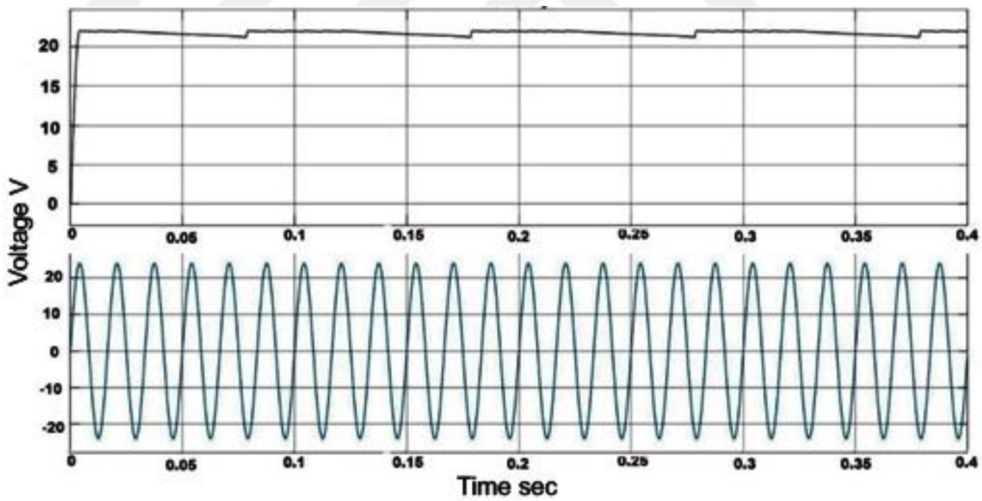

Figure 4.10 The input and output of the AC-DC converter

When an alternating current and voltage enters the circuit, it is converted from alternating wave to direct wave by the alternating signals of a complete rectifier bridge, which can be calibrated to a specific load (battery) to ensure the stabilization of the battery charging voltage as the input changes (the used converter is Buck), which will revile the current value will be negative due to the inversion of the alternating current to direct current.

4.4 DC Buck Converter

Before the signal reaches the battery, it must be tuned to an ideal state following its transformation by the rectifier. To achive that the parameters of the buck converter as in the table 4.1 bellow. In the static case, when a battery is being charged in a stable state without burden and without dynamic external effects such as lighting, the buck converter is a system that converts a signal into its ideal state after it has been rectified. It has several parameters, such as source voltage, load resistance, filter inductor, filter capacitor, duty cycle, and switching frequency. The definition of the transfer function is $(V_{out})/V_{IN}$. The open-loop transfer function must have sufficient gain and phase margins to assure stability and a good transient response as shown in Figure 4.11.

Table 4.1 The buck converter parameters

Source voltage	26 V
Load resistance	1.4 ohm
Filter inductor	1 mH
Filter capacitor	0.1 F
The duty cycle of switch D	1.1
Switching frequency	10 kHz

After defining the buck converter, the transfer function is given as follows:

$$\frac{\Delta V_{out}}{V_{IN}} = \frac{\Delta D/LC}{s^2+\frac{1}{RC}s+\frac{1}{LC}} = \frac{11000}{s^2+0.67s+1*10^4} \tag{4.3}$$

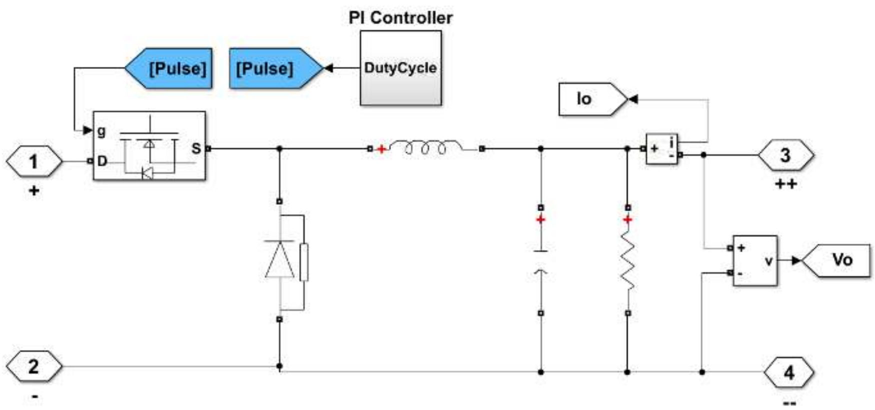

Figure 4.11 Buck converter with PID controller

The system we analyzed in the previous Figures is considered Table because of the small value of phase margin at the crossover frequency, but the gain margin equals infinity, which means that the system is always Table. The transfer function in the open-loop should be designed to give adequate gain and phase margins to guarantee the stability of the system and a good transient response.

4.4.1 PI regulator

The temporal expression of a PI controller is given by Equation (4.4)

$$u(t) = K_p e(t) + K_i \int_0^{\tau} e(\tau) d\tau \tag{4.4}$$

Where $u(t)$ denotes the control signal and $e(t)$ denotes the error. K_p : represents proportional gain and K_i represents the integral gain.

- Tunning of the PI

1. Firstly, we set Ki value to zero.
2. Then elevate Kp until you have the desired system response.
3. Add an integral gain Ki and modify its value until the steady-state error is nullified.

PI controller of Buck converter as shown in Figure 4.12.

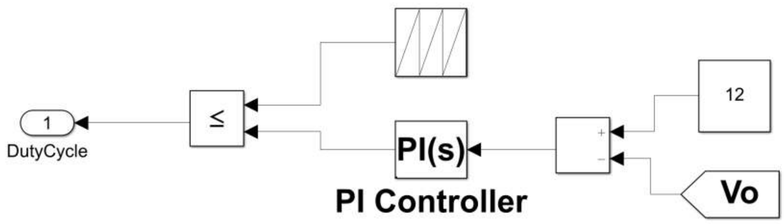

Figure 4.12 Buck converter with PID controller

The controlled voltage for $K_p = 0.1, K_i = 10$

As shown in Figure 4.13 the output voltage of the controlled buck converter.

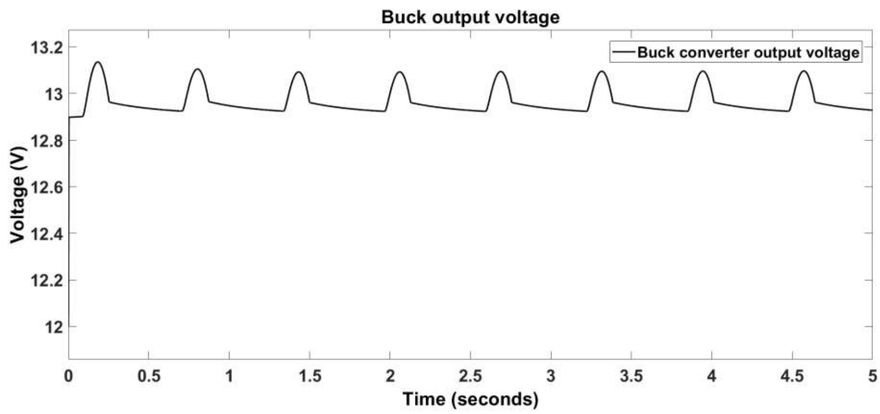

Figure 4.13 Buck converter-controlled output

4.5 Battery

The battery parameters that used in this study shows in Figure 4.14

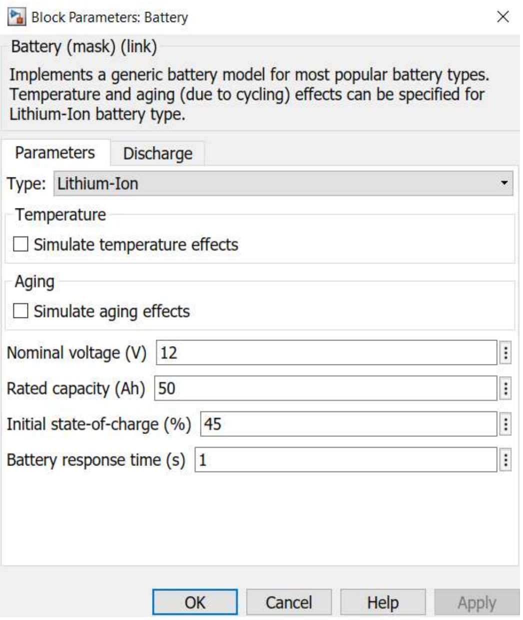
Block Parameters: Battery

Battery (mask) (link)

Implements a generic battery model for most popular battery types. Temperature and aging (due to cycling) effects can be specified for Lithium-Ion battery type.

Parameters | Discharge

Type: Lithium-Ion

Temperature

☐ Simulate temperature effects

Aging

☐ Simulate aging effects

Nominal voltage (V) 12

Rated capacity (Ah) 50

Initial state-of-charge (%) 45

Battery response time (s) 1

OK | Cancel | Help | Apply

Figure 4.14 Lithium-Ion battery parameters

Also, in Figures 4.15, 4.16 and 4.17 the output of the system in the static mode is only charging inspite of the apsence of any load with a surtin amount of voltage and current.

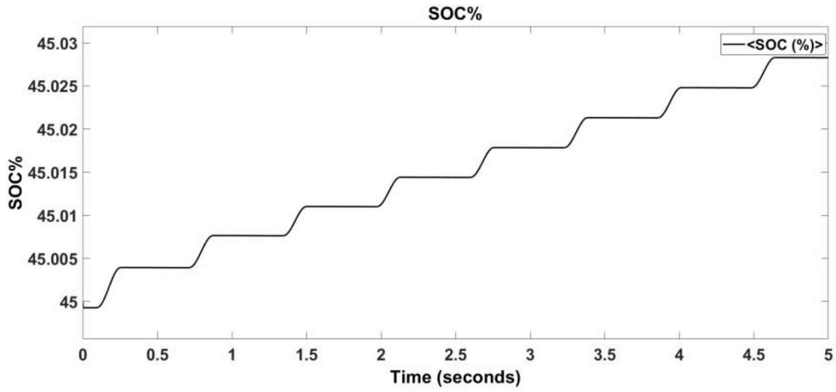

Figure 4.15 Battery state of charge for popoesed system

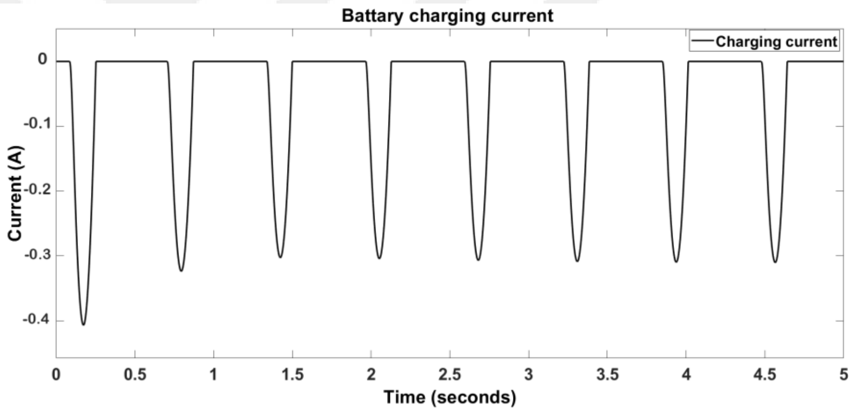

Figure 4.16 Battery current

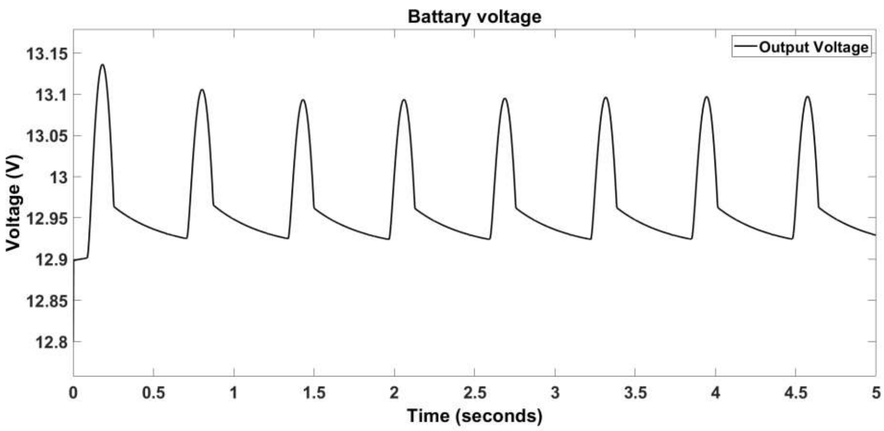

Figure 4.17 Battery voltage

The power output of the system is measured at 3.83 W per pulse, while the height of the speed breaker is recorded at 12cm. This data was collected at a park located in ÇANKIRI. Additionally, the average number of vehicles going over the speed bump on a daily basis in this park is estimated to be 550 cars. The generated power is shown in Table 4.2.

Table 4.2 Amount of generated power

Duration	Generated power
In one hour	229.454 W
In one day	2106.5 W
In one week	16.086 kW
In one month	64.344 kW
In one year	772.128 kW

The information that can be found in Table 4.3 refers to the power generation capacity, the cost of energy generation per hour, and an examination of the annual expenses that are linked with the system.

Table 4.3 Techno-economic analysis of the system

	At the Park
Power generation capacity	0.3 kW/h
Cost of electricity generation per hour	0.0022 kW/h
Annual expenses	$ per kW/h

5. CONCLUSION

This thesis demonstrates an approach to energy generation and conservation by harnessing the energy typically wasted when vehicles pass over speed bumps. Utilizing a double-sided rack and pinion system, an AC generator, and an AC-DC converter, we transformed kinetic energy into storable electrical power. Through meticulous modeling and simulation using MATLAB, our system has proven to be both effective and efficient, producing approximately 772.128 kW annually. These results showcase our technique's potential to generate substantial energy, contributing to the ever-growing demand for power in a manner that's safe and environmentally responsible. The refined DC voltage regulation system and battery charging process ensure optimal storage and utilization of the generated electric power. The success of our system lies not only in energy generation but also in its potential application: illuminating streetlights at night. Road signs are strategically placed throughout its one-kilometer stretch, presenting a sustainable solution to urban power demand challenges. Given the energy crisis, increasing population, and diminishing conventional energy sources, there's a need for innovative solutions like the one proposed in this study. This technology can boost electricity generation within the traditionally power system.

In the future, it will be possible to enhance the system by connecting multiple generators to the branches. This connection will increase the capacity with each passage of vehicles. Additionally, there will be an emphasis on directly using the generated energy, bypassing the need for storage. It has been suggested that specially designed charging stations for electric and hybrid vehicles could harness the energy produced by fossil fuel-powered vehicles in motion. This would then provide power to eco-friendly electric cars. Beyond its primary function within the system, the generated electricity could also recharge electric vehicles. Furthermore, this design has the potential to power traffic lights, charge vehicles, and supply free energy.

REFERENCES

Abdalla, A. N., Nazir, M. S., Tao, H., Cao, S., Ji, R., Jiang, M. and Yao, L. 2021. Integration of energy storage system and renewable energy sources based on artificial intelligence: An overview. Journal of Energy Storage, 40: 102811.

Abdelmalek, S., Dali, A., Bakdi, A.and Bettayeb, M. 2020. Design and experimental implementation of a new robust observer-based nonlinear controller for DC-DC buck converters. Energy, 213: 118816.

Ahamed, Md. A., Reza, M. I. and Al-Amin, Md. 2020. Electricity generation from speed breaker by air compression method using wells turbine. Journal of Advanced Engineering and Computation, 4(2): 140.

Antipin, V. P., Durmanov, M. Ya. and Mikhailov, O. A. 2022. Energy consumption for the utilisation of the tangential traction force in the transport mode of the agricultural machine-tractor aggregate. Lecture Notes in Mechanical Engineering, 247–253.

Azam, A., Aqeeel Aslam, M. and Ali, S. 2016. Speed breaker power generator. Conference: 4th International Conference on Energy, Environment and Sustainable DevelopmentAt: Mehran University of Engineering and Technology.

Baribuma, G., Barinyima, N. 2023. Development and techno-economic analysis of a large-scale speed bump power generation system. International Journal of Sustainable and Green Energy, 12(2):13-20.

Bintu, M. F. B., Ullah, M. W., Hossain, M. I., Faisal, M. M. A. and Rahman, M. F. 2022. Hybrid power generation using speed breaker. 2022 International Conference on Innovations in Science, Engineering And Technology (ICISET).

BUDIMIR, M. Website: https://www.linearmotiontips.com/rack-and-pinion-drives-a-new-look-at-an-old-technology. Date of Access: 15.12.2021.

Chibante, R. and Carvalho, F. 2022. An effective modelling approach for simulation of thyristor rectifiers. 2022 31st Annual Conference of the European Association for Education in Electrical and Information Engineering (EAEEIE).

Dara, J. E., Odazie, C. M., Okolie, P. C. and Azaka, A. O. 2020. Design and construction of a double actuated mechanical speed breaker electricity generator. Heliyon, 6(9): e04802.

Das, S., Das, U. S., Sahoo, A. K., Mishra, S. and Mohapatra, T. K. 2020. Proper harmonic analysis of load current of a single phase 5-level voltage source inverter using HCC. Lecture Notes in Networks and Systems, 195–205.

Dmitriev, D. 2013. Electrıc power generatıng speed bump. Patent Application Publication.

Durai, M. 2017. Using road speed breakers to extract electric power. International Journal of Advanced Research in Basic Engineering Sciences and Technology (IJARBEST), 3: 2395–2695.

Fatima, N. and Mustafa, J. 2016. Production of electricity by the method of road power generation. International Journal of Advances in Electrical and Electronics Engineering, 2319-1112.

Fawade, A. S. 2015. Air Compression and Electricity Generation by Using Speed Breaker with Rack And Pinion Mechanism. International of Modern Engineering Research (IJMER), 2249-6645.

Ionta, A. 2022. E-drives modeling and torque control for electrical vehicles. MSc. Thesis, Politecnico Di Torino University , 112 page, Italy

Ji, F., Wu, D., Li, Y., Zhu, Z. and Zhu, L. 2021. Research on buoy–chain–sprocket wave energy capture technology. Ocean Engineering, 235: 109397.

Kale, A., Naware, U., tandle, P., zulup, M. and Alam, N. 2021. Road Power Generation using Rack and Pinion Mechanism. International Journal of Analysis of Electrical Machines.

Khan, S. A. R., Godil, D. I., Yu, Z., Abbas, F. and Shamim, M. A. 2021. Adoption of renewable energy sources, low-carbon initiatives, and advanced logistical infrastructure—an step toward integrated global progress. Sustainable Development.

Kučera, J., Kováč, J., Palafox, L., Behr, R. and Vojáčková, L. 2020. Characterization of a precision modular sinewave generator. Measurement Science and Technology, 31(6): 064002.

Kushwaha, K., Chaudhary, A. and Dwivedi, A. 2019. Power Generation by Speed Breaker. Journal of Emerging Trends in Electrical Engineering.

Li, J. and Wang, K. 2022. Novel AC-Field Hybrid Excitation DC Generator with Spoke-Type Segmented- PMs Rotor. 2022 IEEE 20th Biennial Conference on Electromagnetic Field Computation (CEFC).

Liu, L., Zheng, W. X. and Ding, S. 2020. An Adaptive SOSM Controller Design by Using a Sliding-Mode-Based Filter and its Application to Buck Converter. IEEE Transactions on Circuits and Systems I: Regular Papers, 67(7): 2409–2418.

Maurya, J., Gupta, P., Gupta, P., Shahab, T. and Amitabh Srivastava, A. S. 2016. Generation of Electricity through Speed Breaker Mechanism. The International Journal of Engineering and Science (IJES).

Minaev, I. V., Tikhonova, I. V., Gvozdev, A. E., Kolmakov, A. G. and Arkhipova, E. A. 2021. Formation of the Cut Surface and the Surface Hardening of Chain Sprockets Made of St3 and 30KhGSA Steels during Laser Cutting. Russian Metallurgy (Metally), 2021(4): 501–506.

Mishra, A., Kale, P. and Kamble, A. 2012. Electricity Generation from Speed Breakers. The International Journal of Engineering and Science (IJES).

Naveen, P., Mukkala, S., Seela, K. R., Arunkumar, Yerra., Teja, B., Mahesh, N., Ganesh, B. Sai., Bhaskar Rao, G. and Ganesh, M. 2022. Design and Fabrication of Power Generation Through Smart Speed Breakers. International Journal for Modern Trends in Science and Technology, 2455-3778.

Padma Rao, A., Kiran Kuma, A. and SureshȦ, S. 2014. Power Generation from Speed Breaker by Rack and Ratchet Mechanism. International Journal of Current Engineering and Technology, 2347 - 5161.

Sai, A. 2021. Free CAD designs, files and 3D models the grabcad community library. Grabcad.com. https://grabcad.com/library/speed-breaker-power-generator-1

Sinha, A., Mittal, S., Jakhmola, A. and Mishra, S. K. 2021. Green energy generation from road traffic using speed breakers. Materials Today: Proceedings, 38, 160–168.

Srivastava, S. and Asthana, A. 2011. Produce electrıcıty by the use of speed breakers. Journal of Engineering Research and Studies.

Wada, T. and Minoru Taya. 2002. Spring-based actuators. In: SPIE's 9th Annual International Symposium on Smart Structures and Materials, 4699.

Xu, M., Han, X., Hua, L. and Zheng, F. 2020. Modeling and methods for gear shaping process and cutting force prediction of variable transmission ratio rack. International Journal of Mechanical Sciences, 171: 105364.

Yan, W., Zhou, J., Peng, Y., Xie, D. and Qu, Y. 2019. Transmission mechanism analysis of downhole drive reciprocating pump production system based on rack and pinion.

Zhang, Y. and Wei, W. 2020. Model construction and energy management system of lithium battery, PV generator, hydrogen production unit and fuel cell in islanded AC microgrid. International Journal of Hydrogen Energy, 45(33): 16381–16397.

APPENDICES

APPENDIX 1. Rack and pinion parameters

Parameter	Data	Results
The outer diameter (Do)	--	40 mm
The No. of Teeth (N)	--	18
The diameter of the pitch circle (D)	Do / (1+2/N) = 40/ (1+2/18)	36 mm
The pinion-angle (Φ)	--	14.5°
Diameter Pitch (P)	N/D = 9/18	0.5 mm
The addendum (a)	1/P	2 mm
Reddendum (b)	1.157/P = 1.157/0.5	2.31 mm
The thickness of the tooth	1.5708/ P = 1.5708 / 0.5	3.14 mm
Formula	Data	Results
The depth of the hole	2.157/P = 2.157/0.5	4.314 mm
The clearance	0.157/ P = 0.157/0.5	0.314 mm
The central distance	((N1 + N2)/ (2*P) = (76 + 18)/ (2* 0.5)	94 mm
The depth	2/P = 2/0.5	4 mm
The diameter of the circle	D + 2m =36 + 2(2)	40 mm

The Calculations are as follows:

(Pitch Circle Diameter/ Number of teeth) = 18/9 = 2 mm.

The radius of pitch circle. (r = 18 mm).

The radius addendum circle (r_a). (r + addendum = 18 + 2 = 20mm).

The pinion angle ((Φ) = 14.5° in volute).

The contact path length $= \frac{a}{\sin\Phi} + \{ra^2 - (r\sin\Phi)^2\}^{\frac{1}{2}} - r\sin\Phi = 13.29$ mm

The contact arc length. (The contact path length / sin Φ = 13.75 mm).

The Min. No. of teeth within a contact. (The contact arc length / π.m = 2).

The pinion angle. (The contact arc length x 360 / $2\pi r_a$ = 39.40°).

The Min. rack Length. ($2\pi r_a$ = 125.660 mm).

APPENDIX 2. Power calculation

In this section, we present the specifications of the components and then calculate the power transmitted through those components. If the proposed system is implemented, it will be necessary to do calculations for certain components in order to assure the system's efficiency and accuracy of the signals.

1. Rack and Pinion Calculation

The Figure 1 shows the rack and pinion parameters also, Table1 illustrated the details.

Table 1. Rack and pinion parameters

The outer diameter (Do)	40 mm
The No. of teeth (N)	18
The diameter of the pitch circle (D)	36 mm
The pinion-angle (Φ)	14.5°
Diameter pitch (P)	0.5 mm
The addendum (a)	2 mm
Reddendum (b)	2.31 mm
The thickness of the tooth	3.14 mm
The depth of the hole	4.314 mm
The clearance	0.314 mm
The central distance	94 mm
The depth	4 mm
The diameter of the circle	40 mm

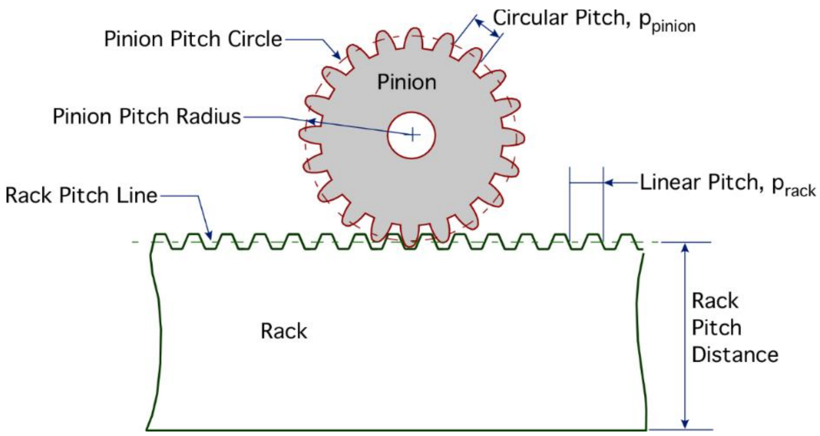

Figure 1 Rack and pinion parameters

Parameters are shown in Table 2

Table 2. System design parameters

Pitch circle diameter/ Number of teeth	2 mm
Radius of pitch circle	18 mm
Radius addendum circle (r_a)	20mm
Pinion angle (Φ)	14.5° in volute
Contact path length	13.29 mm
Contact arc length	13.75 mm
Min. No. of teeth within a contact	2
Pinion angle	39.40°
Min. rack length	125.660

2. Chain Sprocket

The chain sprocket is a power transfer mechanism with a specific speed ratio. It is better to use the volute teeth profile to adjust linear misalignments. And it has to provide higher shock-absorbing capability. The specifications of the gear as shown in Table 3.

Table 3. The specifications of the gear

Outer diameter (Do)	155 mm.
The NO. of teeth (N)	76
Diameter of the pitch circle (D).	151 mm
Gear angle (Φ)	14.5°
Pitch diameter (P)	0.50 mm
Addendum (a)	2 mm
Thickness of the tooth	3.14 mm
Depth of the hole.	4.314 mm
Central distance	94 mm
Depth	4 mm
Diameter of the addendum circle	154.960 mm
Diameter of the Dedendum circle	146.50

The power to be transferred to the AC shaft - Power = 0.180 KW.

- The gear No. of teeth (z2) = 76.
- The pinion No. of teeth (z1) = 18.
- The gear-speed (n2) = 70 rpm.
- The pinion-speed (n1) = 280 rpm.
- The speed ratio (i) = n1/n2 = Z2/Z1 = 4.

3. Design parameters

a) The load of the tangential tooth Equation (4.1)

$$\mathrm{Ft} = 9550 * 1000 * \mathrm{P} * \mathrm{Cs}/\mathrm{n}_1\mathrm{r}_1$$
$$= 9550 * 1000 * 1.22 * 1.5/1120 * 18\mathrm{m} \quad (1)$$
$$= 866.880 \text{ per m}$$

b) Tangential tooth load Lewis Equation (4.2) and (4.3).

$$F_t = \sigma_0 bypK_v \quad (2$$

$$F_t = 137 * 10m * 0.086\,\pi\, m\, K_v = 370.14\, m^2 K_v \quad (3)$$

Where width (b) = 10 m; Pitch (p) = π m

The average speed of the pitch line of the weakest component as shown in the Table 4

Table 4. The average speed of the pitch line

Trials	Selected module	Formula
1st trial	m = 1 mm	$v_m = 1.055 * 1 = 1.055 m/s$
		$K_v = 3/3 + v_m = 0.739$ (velocity factor)
2nd trial	m = 1 mm	$v_m = 1.055 * 1 = 1.055 m/s$
		$K_v = 3/3 + v_m = 0.739$ (velocity factor)

c) Check for the stress

d) Allowable Stress

$$\sigma_{al} = (\sigma_{01} K_v)_{al} = 137 * 0.58 = 79.46 \mathrm{N/mm^2} \quad (4)$$

e) Induction Stress given by Equation (5)

$$\sigma_{1,di} = (\sigma_{01}K_1)_{1,di} = F_t/by_1p = [866.88/2]/(10*2)*(0.086)*2\pi = 40.1\mathrm{N/mm^2} \tag{5}$$

As a result, $(\sigma_{01}K_v)_{1nd} < (\sigma_{01}K_v)_{all}$ so the design is safe.

d) Identification of the weakest component.

The factor of Lewis equals

For 14.5° in volute y = 0.124 – 0.684/z.

For pinion y1 = 0.124 – 0.684/ z1 = 0.124 - 0.684/18 = 0.086.

For gear y2 = 0.124 – 0.684/ z2 = 0.124 - 0.684/76 = 0.115.

The maximum allowable stress value for pinion & gear σ_o = 137 MPa.

$\sigma_o y_1$= (137) (0.086) = 11.78.

$\sigma_o y_2$= (137) (0.115) =15.75

f) Transmitted power to the AC shaft - P = 1.22 KW.

- The teeth No. on gear (z_2) = 76.
- The teeth No. on pinion (z_1) = 18.
- The gear speed (n_2) = 280 rpm.
- The pinion speed (n_1) = 1120 rpm.
- The speed ratio (i) = $n_1/n_2 = Z_2/Z_1$ = 4.

g) Shaft supports gears and flywheels

Using the torsion Equation (6) and (7)

$$\frac{T}{J} = \frac{\tau}{r} \quad (6)$$

And

$$T = Force * Radius \quad (7)$$

Where: T is the Transmitted Torque (N-mm), J Inertial Polar Moment of (mm^2), τ Stress (N/mm^2) and r Shaft Radius (mm).

A generated power would be calculated for this parameters:

- The average mass of a vehicle = 195 Kg.
- The high of speed breaker is 12cm.

So, the weight of the vehicle = m*g = 195Kg * 9.81 m/s^2 = 1912.95 N.

The force which applied on the system of generation electricity = the weight of the vehicle, and the work done = The force * The high of speed breaker

For one push force:

W = 1912.95 * 0.12 / 60 = 3.83 Watts.

Power developed for one vehicle passing over the speed breaker arrangement for push = 3.83 watts.

Based on a survey conducted in one of the parks in ÇANKIRI, it has been observed that the average daily vehicle count amounts to approximately 550. On a weekly basis, approximately 4.100 vehicles are passing over the system in that park.

So, the power that will be generated in one day = 3.83 * 550 = 2106.5 Watts.

Power developed for one week = 16.086 kW.

Power developed for one month = 64.344 kW.

Power developed for one year = 772.128 kW.

CURRICULUM VITAE

Personal Information

Name and Surname : Manar Alaa Khudhur AL-OBAIDI

Education

MSc	Çankırı Karatekin University Graduate School of Natural and Applied Sciences Department of Electric and Electronic Engineering	2020-2023
Undergraduate	University of Diyala Faculty of Engineering Department of Power and Electrical Machine	2008-2012